Studies on Biodegradable Stereocomplex Nanoparticle Composed of Enantiomeric Poly(γ-glutamic acid)-*graft*-poly(lactide) Copolymers as a Protein Delivery Carrier

YE ZHU

Department of Applied Chemistry
Graduate School of Engineering
Osaka University

March 2014

CONTENS

Chapter 3

Biodegradable Nanoparticles Composed of Enantiomeric γ-PGA-*g*-PLA Copolymers as Vaccine Carriers

General Introduction

Vaccination to induce an adaptive immune response is expected for a broad range of infectious diseases and cancers. Traditional vaccines are mainly composed of live attenuated viruses, whole inactivated pathogens, or inactivated bacterial toxins. In general, these approaches have been successful for developing vaccines that can induce an immune response based on antigen-specific antibody and cytotoxic T lymphocyte (CTL) responses, which kill host cells infected with intracellular organisms.[1,2] One of the most important current issues in vaccinology is the need for new adjuvants (immunostimulants) and delivery systems. Many of the vaccines currently in development are based on purified subunits, recombinant proteins, or synthetic peptides. These new generation vaccines are generally very safe, with well-defined components. However, these antigens are often poorly immunogenic, and thus require the use of adjuvants and delivery systems to induce optimal immune responses.[3-5] Immunological adjuvants were originally described by Ramon as "substances used in combination with a specific antigen that produced a more robust immune response than the antigen alone".[6] Until recently, the hydroxide and phosphate salts of aluminum and calcium were the only adjuvants licensed for human use. However, the use of alum-type adjuvants for vaccination has some disadvantages.[7,8] They are not effective for all antigens, induce local reactions, induce IgE antibody responses, and generally fail to induce cell-mediated

immunity, particular CTL responses. Therefore, there is a great need to develop novel immune adjuvants and delivery systems for the next generation of vaccines.[9] Besides immune potentiators, materials that have been investigated as immune adjuvants are nanoparticles (NPs) based vaccine-delivery systems. Polymeric NPs fabricated from biodegradable amphiphilic copolymers are being widely explored as antigen carriers for controlled delivery of different agents including proteins, peptides, and plasmid DNA.[10 - 19] By associated with polymeric NPs, the antigen-uptake efficiency by antigen presenting cells (APCs) is enhanced. More importantly, particulate antigens have been shown to be more efficient than soluble antigens for the induction of immune responses. Therefore, the use of biodegradable polymeric NPs with entrapped antigens represents an exciting approach for controlling the release of vaccine antigens and optimizing the desired immune response via selective targeting of the APCs.[20,21] In a previous study, biodegradable NPs composed of poly(γ-glutamic acid) (γ-PGA) conjugated with L-phenylalanine (Phe) (γ-PGA-Phe NPs) were prepared for the development of safe and effective NP-based vaccines. The antigen encapsulated into γ-PGA-Phe NPs was efficiently taken up by the APCs, and an antigen specific immune response was effectively induced.[22-27] However, although the γ-PGA-Phe NPs could be hydrolytically depredated, the degradation profiler of NPs and antigen releasing behavior was difficult to control.

In this thesis, instead of hydrophobic amino acid, poly(lactide) (PLA), a biodegradable polyesters has been selected as the hydrophobic side chain of the amphiphilic copolymers. By employing stereocomplexation of PLA isomers, a new kind of antigen delivery vehicle with higher thermodynamic and kinetic stability were successfully prepared from the self-assembly of enantimeric poly(γ-glutamic acid)-*graft*-poly(lactide) (γ-PGA-*g*-PLA) graft copolymers. Moreover, the intracellular degradation profilers of NPs and releasing/degradation behavior of encapsulated antigens can also be regulated by changing the physical propriety, crystallinity of the NPs core. Therefore, the NP-based adjuvants may possess the ability to modulate the type of immune responses. It is possible that γ-PGA-*g*-PLA stereocomplex NPs could provide a novel protein-based vaccine capable of inducing strong cellular immunity.

This thesis includes 3 chapters as follows:

In Chapter 1, the amphiphilic graft copolymers, γ-PGA-*g*-PLLA and γ-PGA-*g*-PDLA, consisting of a hydrophilic backbone of γ-PGA and hydrophobic side chains of enantiomeric PLLA or PDLA, were synthesized. The number of enantiomeric PLA chains coupled onto γ-PGA can be controlled by changing the molar amount of PLA added into the reaction system. These γ-PGA-*g*-PLA copolymers could form NPs, and stereocomplex crystallites were formed in the case of the mixture of γ-PGA-*g*-PLLA and γ-PGA-*g*-PDLA copolymers having a relatively large number of PLA grafts.

In Chapter 2, the effects of the molecular weight of the hydrophilic γ-PGA main chain and the grafting degree of the hydrophobic PLA side chain for the formation, stability and crystallinity of NPs formed by isomers and the equal molar mixture of the isomers were investigated. The crystallinity of sterocomplex NPs can also be enhanced by using different preparation method. It is shown that stereocomplex NPs formed from acetonitrile have a higher crystallinity. Expected as a potential delivery system, the loading of model protein Ovalbumin (OVA) into both the isomeric NPs and stereocomplex NPs were successfully achieved by both surface immobilization and physical encapsulation method.

In Chapter 3, the efficacy of γ-PGA-*g*-PLA stereocomplex NPs on cellular uptake, intracellular degradation of protein encapsulated into the NPs *in vitro* and immune induction of protein-encapsulated stereocomplex NPs *in vivo* were investigated. The prepared OVA-encapsulated γ-PGA-*g*-PLA stereocomplex NPs can efficiently taken up by dendritic cells (DCs), and also affected the intracellular degradation of the encapsulated OVA. The degradation of OVA encapsulated into the stereocomplex NPs was attenuated as compared to free OVA and the corresponding isomer NPs. Interestingly, immunization with OVA stereocomplex NPs predominantly induced antigen-specific cellular immunity.

References

1. Z. Zhao, K. W. Leong, *J. Pharm. Sci.* **1996**, *85*, 1261.

2. M. Singh, D. T. O'Hagan, *Pharm. Res.* **2002**, *19*, 715.

3. M. Singh, D. T. O'Hagan *Nat. Biotechnol.* **1999**, *17*, 1075.

4. D. T. O'Hagan, R. Rappuoli *Pharm. Res.* **2004**, *21*, 1519.

5. L. J. Peek, C. R. Middaugh, C Berkland, *Adv. Drug Deliv. Rev.* **2008**, *60*, 915.

6. G. Ramon, *Ann. Inst. Pasteur.* **1924**, *38*, 1.

7. R. K. Gupta, *Adv. Drug. Deliv. Rev.* **1998**, **32**, 155.

8. J. M. Brewer, *Immunol. Lett.* **2006**, *102*, 10.

9. M. O. Oyewumi, A. Kumar, Z. Cui, *Expert Rev. Vaccines* **2010**, *9*, 1095.

10. K. Letchford, H. Burt, *Eur. J. Pharm. Biopharm.* **2007**, *65*, 259.

11. C. Cai, J. Lin, T. Chen, X. Tian, *Langmuir* **2010**, *26*, 2791.

12. S. J. Holder, N. A. J. M. Sommerdijk, *Polym. Chem.* **2011**, *2*, 1018.

13. J. S. Lee, J. Feijen, *J. Controlled Release* **2012**,*161*, 473.

14. J. Z. Du, L. Fan, Q. M. Liu, *Macromolecules* **2012**, *45*, 8275.

15. S. Chen, S. Cheng, R. Zhuo, *Macromol. Biosci.* 2011, *5*, 576.

16. Y. Krishnamachari, S. M. Geary, C. D. Lemke and A. K. Salem, *Pharm. Res.* **2011**, *28*, 215.

17. S. Chen, S. X. Cheng and R. X. Zhuo, *Macromol. Biosci.* **2011**, *11*, 576.

18. A. Rösler, G. W. Vandermeulen and H. A. Klok, *Adv. Drug Deliv. Rev.* **2012**, *64*, 270.

19. Y. Ohya, A. Takahashi, K. Nagahama, *Adv. Polym. Sci.* **2012**, *247*, 65.

20. T. Akagi, M. Baba, M. Akashi, *Adv. Polym.Sci.* **2012**, *247*, 3.

21. D. T. O'Hagan, N. M. Valiante, *Nat. Rev. Drug Discov.* **2003**, *2*, 727.

22. T. Akagi, M. Baba, M. Akashi, *Polymer* **2007**, *48*, 6729.

23. H. Kim, T. Akagi, M. Akashi, *Macromol. Biosci.* **2009**, *9*, 825.

24. T. Akagi, T. Kaneko, T. Kida, M. Akashi, *J. Controlled Release* **2005**, *108*, 226.

25. Akagi, T., Wang, X., Uto, T., Baba, M., and Akashi, M. *Biomaterials* **2007**, *28*, 3427.

26. X. Wang, T. Uto, K. Sato, K. Ide, T. Akagi, M. Okamoto, T. Kaneko, M. Akashi, M. Baba, *Immunol. Lett.*, **2005**, *98*, 123.

27. T. Uto, X. Wang, K. Sato, M. Haraguchi, T. Akagi, M. Akashi and M. Baba, *J. Immunol.*, **2007**, *178*, 2979.

Chapter 1

Synthesis of Enantiomeric γ-PGA-*g*-PLA Copolymers and Preparation of Stereocomplex Nanoparticles

1.1 Summary

Novel amphiphilic graft copolymers composed of poly(γ-glutamic acid) (γ-PGA) as a hydrophilic backbone and enantiomeric poly(lactide) (PLA) as hydrophobic side chains were successfully synthesized. The number of poly(L-lactide) (PLLA) or poly(D-lactide) (PDLA) chains grafted onto the γ-PGA main chain was enhanced by increasing the feed ratio of PLA to γ-PGA in the reaction system. Enantiomeric and stereocomplex nanoparticles (NPs) self-assembled from isomeric γ-PGA-*g*-PLLA or γ-PGA-*g*-PDLA copolymers and equal molar mixtures of enantiomeric γ-PGA-*g*-PLLA and γ-PGA-*g*-PDLA copolymers were formed in aqueous solution. The mean diameters of the both the isomeric and stereocomplex NPs can be controlled by changing the γ-PGA main chain length and grafting degree of PLA side chain. Furthermore, these NPs with reactive functional groups would have great potential to be used as stable delivery vehicles for pharmaceutical and biomedical applications.

1.2 Introduction

Nanostructures prepared from the self-assembly of amphiphilic block or graft copolymers in aqueous solution have attracted widespread attention in the biomedical and pharmaceutical fields.[1]-[4] In particular, spherical micelle-like nanoparticles (NPs) composed of hydrophobic inner cores and hydrophilic shells have been extensively studied over the past decade as delivery vehicles for chemical therapies.[5]-[9] As a delivery vehicle, the one remaining challenge for particle-based delivery systems is the inferior *in vivo* stability.[10] Normally chemical cross-linking is adapted to improve NPs stability, but the use of cross-linkers may unfavorably affect the bioactivity of the encapsulated cargo and the biodegradability of the delivery system.[11] Therefore, stabilization of the particle core through physical interactions such as stereocomplexation is an alternative strategy.

Stereocomplexation between the L and D type enantiomers of PLA are the most commonly investigated not only due to their biodegradability and biocompatibility, but also because they are hydrolysable in the human body as well as in each environment. In the previous studies, poly(L-lactide)/poly(D-lactide) (PLLA/PDLA) containing copolymers of various architectures were synthesized to form stereocomplex self-assemblies.[12]-[16]

However, the majority of the researches performed on the formation of NPs through stereocomplexation between PLA enantiomers are based on polymers without reactive functional groups as a side chain, while preparation of stereocomplex NPs through biodegradable copolymer systems and their applications as delivery system were seldom reported.

Poly(γ-glutamic acid) (γ-PGA), a naturally occurring water soluble poly(amino acid) has been considered as a unique properties for biodegradability, immunogenicity, and immunoreactivity.[17],[18] In a previous study from our group, size-controllable NPs which can be used as an effective vaccine delivery system, was prepared using a hydrophobic amino acid (L-phenylalanine ethylester, Phe) modified γ-PGA-*graft*-Phe (γ-PGA-Phe) copolymer.[19]-[23] NPs composed of amphiphilic γ-PGA-Phe with a greater than 50% grafting degree of Phe could covalently immobilize proteins and peptides *via* carboxyl groups located on the NP surfaces.[24],[25] However, the γ-PGA-Phe NPs still have some problems for *in vivo* applications, such as a relatively low drug-loading efficiency on the surfaces and difficulty in controlling the degradation process. In order to improve these drawbacks, other types of hydrophobic groups or biodegradable hydrophobic polymers, such as PLA, should be employed as the hydrophobic part to modify the γ-PGA main chains through the functional carboxyl groups. γ-PGA contains multiple carboxyl groups, and have therefore found utility as hydrophilic and

bioactive segments in some hybrid biomaterials. One promising approach to regulate the hydrophobicity of γ-PGA with low degree of substitution is the introduction of hydrophobic polymers. It is considered that the hydrophilic-hydrophobic balance can be easily modulated as a function of the degree of substitution (grafting degree) and the degree of polymerization. The graft copolymer structure may provide integration of considerable functionality onto the polymer backbone that can be addressed chemically after the assembly process. In this chapter, we developed a method to modify γ-PGA by hydrophobic PLA homopolymers and the characterization of comb-like amphiphilic γ-PGA-*graft*-PLLAs (γ-PGA-*g*-PLLA) and γ-PGA-*g*-PDLAs were investigated. The capability of forming polymer nanoparticles in aqueous solution and the ability of stereocomplex formation between γ-PGA-*g*-PLLA and γ-PGA-*g*-PDLA were discussed

1.3 Experimental Section

Materials

L-lactide and D-lactide were purchased from Purac Biochem BV (Gorinchem, the Netherlands) and were re-crystallized twice from ethyl acetate prior to use. Poly(γ-glutamic acid) (γ-PGA, number average molecular weight, M_n = 75 kDa, molecular weight distribution, M_w/M_n = 2.0), decanol ($C_{10}H_{21}OH$), stannous

octanoate [$Sn(Oct)_2$], tetrahydrofuran (THF), dimethyl formamide (DMF), chloroform and other chemicals were purchased from Wako Pure Chemical Industries (Tokyo, Japan). Anhydrous toluene, anhydrous dimethyl sulfoxide (DMSO) and anhydrous 1,4-dioxane used as reaction solvent were purchased from Wako Pure Chemical Industries (Tokyo, Japan), and were used without further purification. *N*-Boc-ethanolamine (Boc: *t*-butoxycarbonyl), 1-ethyl-3-(3-dimethylaminopropyl)-carbodiimide (EDC) and 4-(*N*,*N*-dimethylamino)pyridine (DMAP) were purchased from Sigma (St. Louis, MO), and were used as received.

Synthesis of hydroxyl- and amine-terminated enantiomeric PLLA and PDLA

Hydroxyl- and amine-terminated PLAs were prepared by the ring-opening polymerization of L- and D-lactides using decanol and *N*-Boc-ethanolamine as an initiator, followed by deprotection.[26] Taken preparation of amine-terminated PLAs as an example, monomeric L or D-lactide (5 g, 34.7 mmol), *N*-Boc-ethanolamine (0.33 g, 2.04 mmol) and anhydrous toluene (10 mL) were charged into a flame-dried flask, followed by three vacuum-nitrogen cycles. Then 1 mL of $Sn(Oct)_2$ in toluene (1 mol/L) was added under nitrogen protection. The reaction mixture was stirred at 120°C for 4 h. The obtained polymer was isolated by pouring the reaction mixture into an excess amount of diethyl ether, and further purified by repeated precipitation. The final product was dried under

vacuum at room temperature overnight to give a white solid with a yield of 75%. Gel permeation chromatography (GPC; chloroform, 1.0 mL/min) revealed that Boc-NH-PLLA had a M_n of 2.6 kDa, and M_w/M_n of 1.3, whereas Boc-NH-PDLA had a M_n of 2.5 kDa and M_w/M_n of 1.3.

The degree of polymerization (DP) of Boc-NH-PLLA and Boc-NH-PDLA were determined by proton nuclear magnetic resonance (^{1}H NMR) spectroscopy to be 36 and 34, respectively, as follows: ^{1}H NMR ($CDCl_3$): δ (ppm) = 1.44 (s, 9H, $CH(CH_3)_3$ of the Boc group), 1.57-1.59 (d, 3H, $CHCH_3$ of PLA), 3.37-3.39 (br, 2H, NCH_2CH_2O), 4.15-4.23 (br, 2H, NCH_2CH_2O), 4.34-4.37 (q, 1H, terminal-$CHCH_3$), 5.14-5.18 (q, 1H, $CHCH_3$ of PLA). The removal of the protection group from the PLA-NH-Boc was carried out by treatment in a mixed solvent of formic acid (20 mL) and $CHCl_3$ (20 mL) for 8 h, followed by treatment in a mixed solvent of triethylamine (TEA; 20 mL) and $CHCl_3$ (20 mL) to deprotonate at room temperature for another 8 h. The obtained polymer was isolated by pouring the mixture into an excess amount of diethyl ether, and was further purified by repeated precipitation. The final product was dried under vacuum at room temperature overnight The removal of the Boc group was confirmed by ^{1}H NMR as follows: ^{1}H NMR ($CDCl_3$): δ (ppm) = 1.57-1.58 (d, 3H, $CHCH_3$ of PLA), 3.41-3.43 (q, 2H, NCH_2CH_2O), 3.70-3.72 (t, 2H, NCH_2CH_2O), 4.34-4.37 (q, 1H, terminal-$CHCH_3$), 5.14-5.18 (q, 1H, $CHCH_3$ of PLA).

Hydrolysis and analysis of γ-PGA

Commercially-available γ-PGA (M_n = 75 kDa, M_w/M_n = 2.0) was hydrolyzed in 1 M and 2M NaOH aqueous solution at 80°C for 8 h with shaking. In order to collect the low molecular weight γ-PGA, the solution was acidified with 5 M HCl. After acidification, the samples were kept at 4°C until the low molecular weight γ-PGA precipitated. In the case of hydrolysis under 2M NaOH, no precipitation was collected. The low-molecular weight γ-PGA was then collected by filtration and vacuum-dried overnight. The molecular weight of the 1M NaOH hydrolyzed γ-PGA was measured by GPC using DMSO as the eluant, revealing a M_n of 10 kDa and M_w/M_n of 1.4.

Synthesis of γ-PGA-g-PLA amphiphilic graft copolymer

Briefly, the γ-PGA-*g*-PLLA and γ-PGA-*g*-PDLA graft copolymers were synthesized by a coupling reaction. γ-PGA (100 mg, 0.775 unit mmol), stoichiometric amounts of EDC (149 mg, 0.775 mmol) and DMAP (95 mg, 0.775 mmol) were dissolved in 10 mL of dehydrated DMSO. Then 1 mL of pre-dissolved PLLA or PDLA/dioxane solution at various concentrations was slowly added into the mixture solution under nitrogen protection. The reaction was allowed to continue for 24 h at 40°C with stirring. The reaction mixture was dialyzed against pure water using a dialysis membrane (molecular weight cut-off 50 kDa) for two days, and lyophilized until dry. The obtained products were

washed twice by an excess amount of THF to remove the uncoupled PLLA or PDLA. The obtained precipitate was then collected by centrifugation, and dried under vacuum overnight. The average number of PLLA or PDLA grafted per γ-PGA chain was determined by ^{1}H NMR analysis in DMSO-d_6 using the integrals of the methylene peaks (2.20 ppm, NHCHCH_2CH$_2$ and 1.74-1.90 ppm, NHCHCH$_2$CH_2) in the γ-PGA backbone and the methine peaks (5.20 ppm, CHCH$_3$ of PLA) in the PLA main chain as. However, when the PLA content in copolymer is higher than 60%, due to the solubility change of γ-PGA-*g*-PLA copolymers in THF, the unconjugated PLAs were difficult to remove and the samples were not able to purify.

Preparation of γ-PGA-g-PLA NPs

Aqueous copolymer NPs were prepared by the dialysis method. Briefly, γ-PGA-*g*-PLLA, γ-PGA-*g*-PDLA and an equal molar mixture of PLLA and PDLA copolymer were first dissolved in DMSO, a solvent for both γ-PGA and PLA, to a concentration of 10 mg/mL. Then, phosphate buffer saline (PBS; 10 mM, pH 7.4, 0.15 M NaCl), which is a non-solvent of PLA, was added dropwise into the copolymer solution with vigorous stirring until the water content reached 50 vol. %. The solutions were transferred into a dialysis tube (MWCO: 1,000 Da) for dialysis against pure water to remove the DMSO. After dialysis, the particle size and distribution were measured by dynamic light scattering (DLS). The

samples for fluorescence and wide angle X-ray diffraction (XRD) measurements were prepared by lyophilization.

Characterization methods

^{1}H NMR spectra were recorded with a Varian INOVA-600 instrument. Gel permeation chromatography (GPC) measurements for PLLA and PDLA were measured by a JASCO SEC system (JASCO PU-2080, JASCO RI-2031, and JASCO CO-2065) at 40°C with a TSKgel GMH_{XL} column using chloroform as the eluent at a rate of 0.6 mL/min. PMMA was used for the calibration. The IR spectra were recorded on a Perkin-Elmer Spectrum 100. The particle sizes of the γ-PGA-*g*-PLA NPs in aqueous solutions were measured by dynamic light scattering (DLS) using a Zetasizer Nano ZS (Malvern Instruments, UK) at a wavelength of 633 nm and a detection angle of 173°. The morphology of γ-PGA-*g*-PLA NPs were observed by scanning electron microscopy (SEM) (JSM-6700F, JEOL) at 5 kV. A drop of the NPs suspension was placed on a glass surface, which was fixed on metallic supports with carbon tape. After drying, the samples were coated with osmic acid. The wide-angle X-ray diffraction (XRD) patterns were recorded on a RIGAKU RINT2000 instrument with a Cu K α (λ = 0.154 nm) source at room temperature, and was operated at 40 kV and 200 mA with a Ni filter.

1.4 Results and Discussion

Synthesis of γ-PGA-g-PLA copolymers

As shown in Scheme 1-1, γ-PGA-*g*-PLLA and γ-PGA-*g*-PDLA copolymers were prepared by a two steps reaction. First, the enantiomeric PLLA (M_w = 3,000) and PDLA (M_w = 4,000) homopolymers were synthesized by a ring-opening polymerization of the L-lactide or D-lactide monomer with n-decanol as the initiator and $Sn(Oct)_2$ as the catalyst. The molecular weight and degree of polymerization were both measured by ^1H NMR. Next, graft copolymers with different grafting degree of PLA were synthesized by a coupling reaction between the terminal hydroxyl group in PLA and the carboxylic groups in γ-PGA using EDC. After dialysis against water and lyophilization, the copolymers were washed with THF twice to remove the unconjugated PLA. γ-PGA-*g*-PLA copolymers were precipitated in THF and collected by centrifugation. The characterization of the γ-PGA-*g*-PLLA and γ-PGA-*g*-PDLA copolymers thus obtained is summarized in Table 1-1.

The grafting degree of PLA, the number and hydrophobic content (%) of the PLAs in the copolymer, were calculated from ^1H NMR (solvent DMSO-d_6) using the integrals of the methylene peaks (2.20 ppm a-CH_2 and 1.74-1.90 ppm, b-CH_2) in the γ-PGA backbone and the methine peaks (5.20 ppm e-CH) in the PLA main

chain (Figure 1-1). The number of the PLA chains grafting was controlled by altering the feed ratio between γ-PGA and PLA in the reaction system. By using hydroxyl terminal PLA, due to the low reactivity, the grafting degree of the copolymer was very low. However, it is noteworthy that the grafting degree of the copolymers does increase by changing the feed ratio of PLA to γ-PGA, which demonstrated that the hydrophobic substitution degree of the copolymers can be controlled by altering the amount of PLA feeding into the reaction system. As compared with hydroxyl-terminated PLA, under similar reaction conditions, the content of PLA units in the copolymer increased from lower than 20% to higher than 30%, especially PGA-L_{11} and PGA-D_{12}, in which the hydrophobic content was over 50%. This was mainly due to the usage of amino-terminated PLAs, whose reactivity is much higher than hydroxyl-ended PLAs. It is found that the solubility of high molecular weight PLA (M_n = 5 kDa) in DMSO was very poor, and γ-PGA modified by high molecular weight PLA were easily form precipitations during the self-assembly process. Therefore, γ-PGA-*g*-PLAs with low degree of polymerization PLA (DP = 35) side chains were selected for further study.

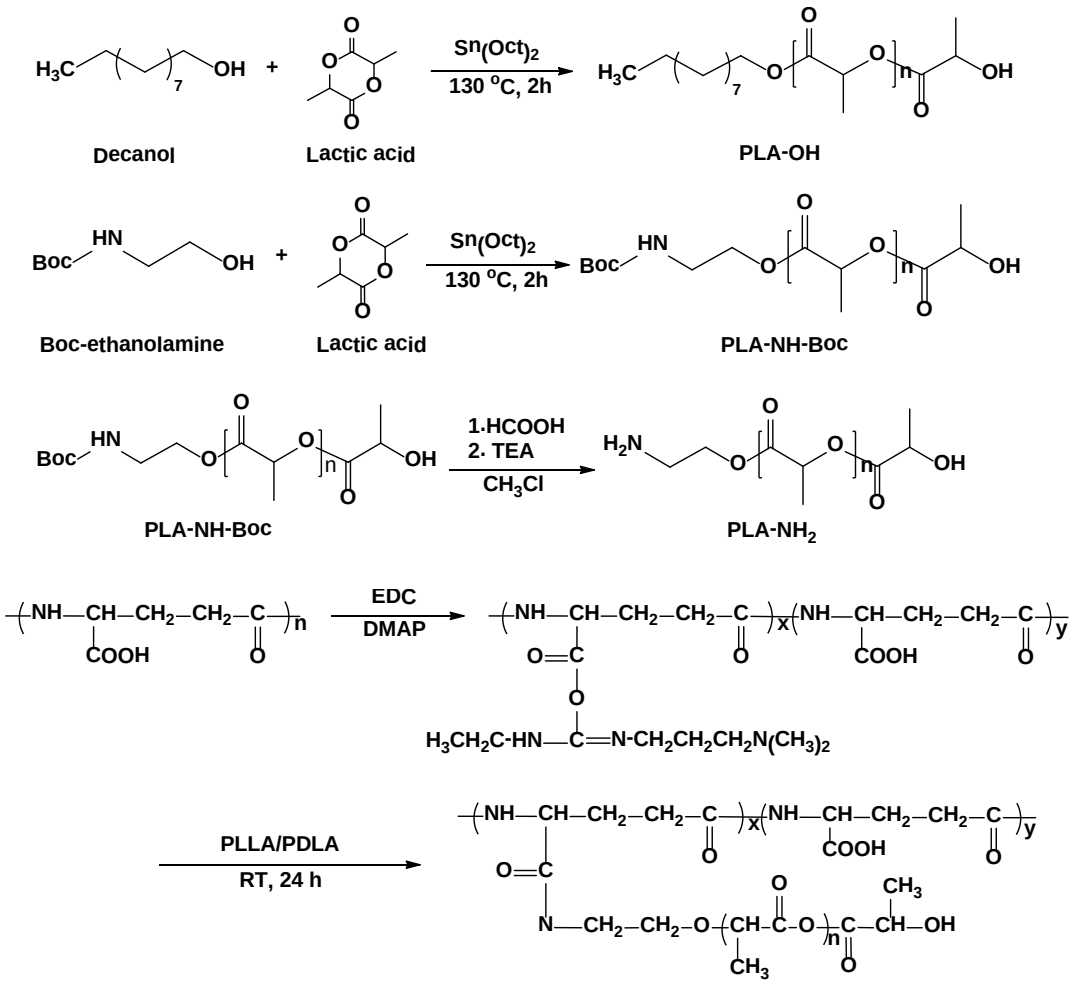

Scheme 1-1. Synthesis of hydroxyl-, amino-terminated PLLA/PDLA polymer and γ-PGA-g-PLLA/PDLA copolymers.

Solubility of γ-PGA-g-PLA copolymers

The solubility of γ-PGA, PLA and the copolymer in water and several common organic solvents were investigated. γ-PGA is known to be soluble in pure water, buffer solution and DMSO, whereas PLA can be dissolved in THF, chloroform, DMF acetonitrile and some other organic solvents. However, all of the γ-PGA-*g*-PLLA and γ-PGA-*g*-PDLA copolymers with different PLA contents were soluble in DMSO, but could not be dissolved in water or other friendly organic solvents for PLA, such as THF, chloroform and DMF. This was probably due to the amphiphilic properties of the copolymer. Although hydrophobic PLAs were connected onto the hydrophilic γ-PGA and the number of PLA chains grafted onto the copolymers were improved by enhancing the feed molar ratio of PLA or changing into PLA with higher reactivity terminal group, the content of the hydrophobic part in the copolymer is still low (mainly lower than 50% except PGA-L_{11} and PGA-D_{12}), and the majority part of the copolymer consisted of γ-PGA, which inhibited the dispersion of the copolymer in common organic solvents.

Table 1-1. Synthesis of γ-PGA-*g*-PLLA and γ-PGA-*g*-PDLA copolymers using

Code	Sample	γ-PGA (mg)	PLA (mg)	Feed Ratio[b]	Yield[c] (%)	Grafting Degree[d] (%)		PLA Content[e] (wt.%)
						In feed	^{1}H NMR	
PGA-L_1	γ-PGA_{75k}-*g*-$PLLA_{0.3}$	100	50	0.5	53	2.5	0.3	10
PGA-D_2	γ-PGA_{75k}-*g*-$PDLA_{0.3}$	100	50	0.5	48	2.5	0.2	10
PGA-L_3	γ-PGA_{75k}-*g*-$PLLA_{0.6}$	100	100	1	50	5.0	0.6	15
PGA-D_4	γ-PGA_{75k}-*g*-$PDLA_{0.5}$	100	100	1	45	5.0	0.5	15
PGA-L_5	γ-PGA_{75k}-*g*-$PLLA_{1.0}$	100	200	2	42	7.5	1.0	20
PGA-D_6	γ-PGA_{75k}-*g*-$PDLA_{0.7}$	100	200	2	38	7.5	0.7	20
[a]PGA-L_7	γ-PGA_{75k}-*g*-$PLLA_{2.6}$	100	200	2	56	7.5	2.6	35
[a]PGA-D_8	γ-PGA_{75k}-*g*-$PDLA_{2.2}$	100	200	2	52	7.5	2.2	30
[a]PGA-L_9	γ-PGA_{10k}-*g*-$PLLA_{3.4}$	100	200	2	53	7.5	3.4	40
[a]PGA-D_{10}	γ-PGA_{10k}-*g*-$PDLA_{3.1}$	100	200	2	57	7.5	3.1	40
[a]PGA-L_{11}	γ-PGA_{10k}-*g*-$PLLA_{7.4}$	100	300	3	26	12.5	7.4	60
[a]PGA-D_{12}	γ-PGA_{10k}-*g*-$PDLA_{6.1}$	100	300	3	28	12.5	6.1	55

[a] Amino-endded PLA samples;

[b] Feed ratio = PLA/γ-PGA (g/g);

[c] Yield = [(γ-PGA-*g*-PLA) / (PLA + γ-PGA)] × 100% (g/g);

[d] Grafting degree and number of grafted PLA chains were estimated by ^{1}H NMR (solvent DMSO-d_6);

[e] PLA content was the content of PLA unit in wt. % = [(M_w of PLA × the number of grafted PLAs) / (M_w of γ-PGA-*g*-PLA copolymers)].

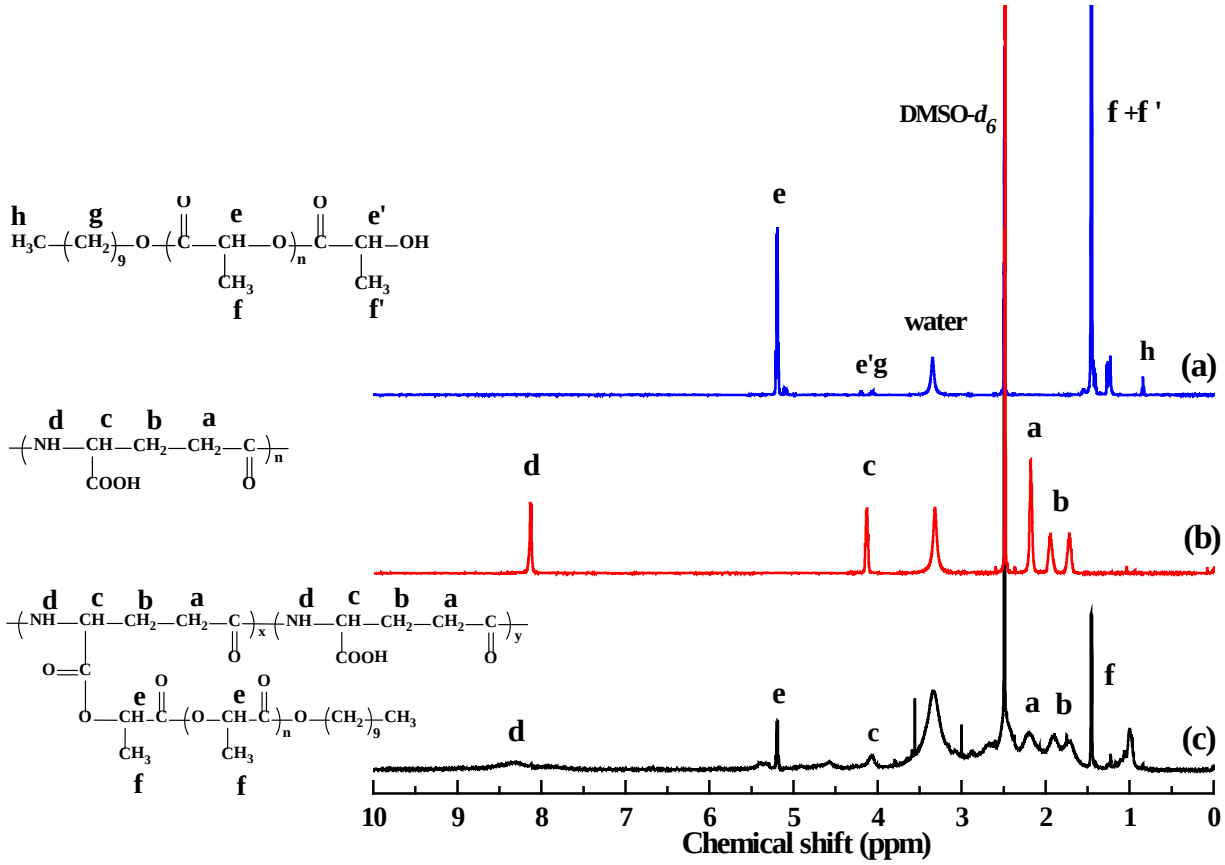

Figure 1-1. ^{1}H-NMR spectra of (a) PLA, (b) γ-PGA, and (c) PGA-L_5 copolymer

Preparation of γ-PGA-g-PLA stereocomplex NPs

γ-PGA-*g*-PLA NPs and stereocomplex NPs were prepared by slowly adding PBS dropwise into DMSO solutions of γ-PGA-*g*-PLLA, γ-PGA-*g*-PDLA and an equimolar mixture of the two under vigorous stirring. The formation of these NPs was accomplished due to the presence of the hydrophobic PLA side chains and the hydrophilic γ-PGA main chain. With the addition of PBS, a poor solvent for the PLA segment, the solubility of the copolymers decreased. In order to minimize the free energy of the system, the free copolymer chains began to associate with each other through hydrophobic interactions between the PLA side chains to form the cores of the NPs, while the hydrophilic part of the copolymer, γ-PGA, dissolved in the buffer to form the NP shells. In the case of stereocomplex NPs, when the equimolar mixture of enantiomeric copolymers came into contact with the non-solvent PBS under stirring, the association of the enantiomeric PLA chains took place very quickly before the solution goes into microscopic phase separation,[27],[28] and finally formed the stereocomplex cores (Scheme 1-2).

To further prove the formation of NPs using γ-PGA-*g*-PLA, ^{1}H NMR spectroscopy of PGA-L_{11} NPs dispersed in DMSO-d_6 and D_2O were carried out. NMR can be employed to study the structure of polymeric NPs, especially for core-shell type particles. Since both γ-PGA and PLA can dissolve in DMSO-d_6

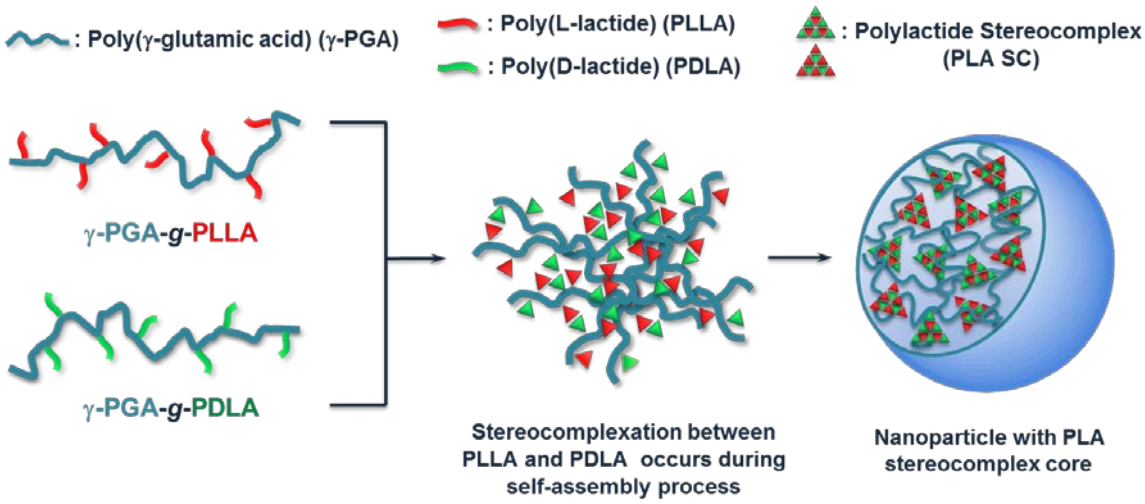

Scheme 1-2. Schematic illustration of NPs formation by the stereocomplexation of γ-PGA-*g*-PLLA and γ-PGA-*g*-PDLA copolymers.

and exist in a liquid state, particle formation was not expected. The characteristic peaks of γ-PGA and PLA are shown in DMSO-d_6.

However, the characteristic NMR peaks of PLA disappeared completely using D_2O. These results indicate that the protons of PLA displayed restricted motion, and have a solid-like structure. The NMR peaks of the hydrophilic γ-PGA chains were detected using D_2O, implying that the structure of NPs consisting of γ-PGA-*g*-PLA should be a core-shell type composed of inner core of PLA and outer shell of γ-PGA. Unlike amphiphilic block copolymers, which are linear and have a higher hydrophobic content, these γ-PGA-*g*-PLA copolymers had a relatively low grafting degree (less than 10%) and preferred to assemble into multicore NPs. Therefore, it is suggested that the interior of the NPs was formed not only by PLA, but also by the main chain γ-PGA.

Their hydrophilic domains are either exposed to the aqueous solvent, or to a low level of hydrophilic domains present within the NPs, whereas the hydrophobic chains associated together as cross linking point to keep the structure intact as an entity. The hydrodynamic diameter (d_h) and distribution index of the NPs were measured by DLS. As an example, the size distributions of NPs fabricated from PGA-L_{11}, PGA-D_{12} and the equimolar mixture of two (SC_{11+12}) are shown in Figure 1-2e. The d_h values of the PGA-L_{11} and PGA-D_{12}

NPs were both determined to be around 300 nm, with low polydispersity. Compared with isomer NPs, SC_{11+12} stereocomplex NPs formed by the mixture of two have a smaller size (around 200 nm), and lower polydispersity. The morphology of the SC_{11+12} stereocomplex NPs was observed by SEM. As shown in Figure 1-2f, the SC_{11+12} stereocomplex NPs were spherical with an average diameter of 170 nm, which was about 40 nm smaller than the size measured by DLS. This reduced diameter can be attributed to the difference between the dried and hydrated states.

Table 1-2 summarizes the size and zeta potential of NPs prepared from a series of copolymers. In general, all the NPs showed a negative zeta potential in PBS. This could be attributed to the presence of ionized carboxyl groups from the γ-PGA on the NPs surfaces. The hydrodynamic diameter polydistribution of all NPs are monodispersed, exhibiting an average intensity ranging from 90 nm to 330 nm (Figure 1-2a-d). These results suggest that the d_h of the NPs increased with the increasing of the PLA grafting degree (e.g. PGA-L_9 and PGA-L_{11}). Moreover, sharing similar grafting degree, the size of NPs formed by copolymers with a longer main chain are much bigger than those assembled from short main chain copolymers (e.g. PGA-L_7 and PGA-L_9). The main chain of the PGA-L_7 and PGA-D_8 copolymers are longer than the PGA-L_9 and PGA-D_{10} copolymers, indicating that the NPs formed by the PGA-L_7 and PGA-D_8 copolymers might

process a loosely aggregation manner and are largely swollen in water. On the other hand, in the PGA-L_9 and PGA-D_{10} copolymers, only two PLA chains are grafted onto the main chain, which means that the structure of these two copolymers are similar to block type copolymers, and that they might prefer to assemble into micelle-like NPs with a higher packing density. In the case of stereocomplex NPs formed by the equalmolar mixture of γ-PGA-*g*-PLLA and γ-PGA-*g*-PDLA, when compared with NPs formed by γ-PGA-*g*-PLA isomers, the sizes of stereocomplex NPs were generally smaller with significantly narrower polydistributions.

Wide-angle X-ray diffraction measurement of γ-PGA-g-PLA NPs

In an attempt to gain insight into the physical state of the copolymer NP cores, wide-angle X-ray diffraction (XRD) studies of the lyophilized NPs were carried out and a stereocomplex. PGA-L_7, PGA-D_8, and stereocomplex of SC-NP_{7+8} were carried out (Figure 1-3). The crystalline peak at 2θ values of 12° and 21° were detected which are characteristic peaks of the PLA stereocomplex (β-form). However, in the case of isomeric or stereocomplex NPs formed by copolymers with lower than 20% of PLA content, no crystalline peaks cannot be detected in both isomeric or stereocomplx NPs, indicating that the core of NPs formed by copolymers only were amorphous. The amount of PLA content in the copolymers played an important role on stereocomplex formation. With increasing PLA

content in the copolymers, stereocomplex NPs yielded relatively clear crystalline peaks at 12° and 21°.

Table 1-2. Characterization of NPs formed by individual and mixed γ-PGA-*g*-PLA copolymers.

Sample	Particle		Zeta Potential[a] (mV)
	d_h [a] (nm)	PDI[b]	
PGA-L_7	260 ± 7.1	0.14 ± 0.01	-18.3 ± 0.3
PGA-D_8	245 ± 7.2	0.20 ± 0.02	-19.5 ± 0.3
[d]SC_{7+8}	190 ± 0.8	0.12 ± 0.04	-20.6 ± 1.3
PGA-L_9	110 ± 4.4	0.12 ± 0.02	-25.6 ± 1.8
PGA-D_{10}	95 ± 2.9	0.13 ± 0.01	-24.1 ± 1.4
[d]SC_{9+10}	90 ± 0.5	0.10 ± 0.01	-26.3 ± 1.5
PGA-L_{11}	330 ± 2.0	0.09 ± 0.01	-26.9 ± 0.8
PGA-D_{12}	300 ± 3.2	0.11 ± 0.03	-28.1 ± 1.7
[d]SC_{11+12}	210 ± 1.7	0.07 ± 0.03	-29.0 ± 1.1

[a] The particle size and zeta potential of individual and stereocomplex γ-PGA-*g*-PLA NPs were measured in PBS at 1 mg/mL (mean ± SD of three independent experiments is shown);

[b] Polydispersity index;

[c] SC means stereocomplex formed by the equal molar mixture of PGA-L and PGA-D, e.g. SC_{1+2} means stereocmplex NPs formed by the mixture of PGA-L_1+PGA-D_2 et cetera;

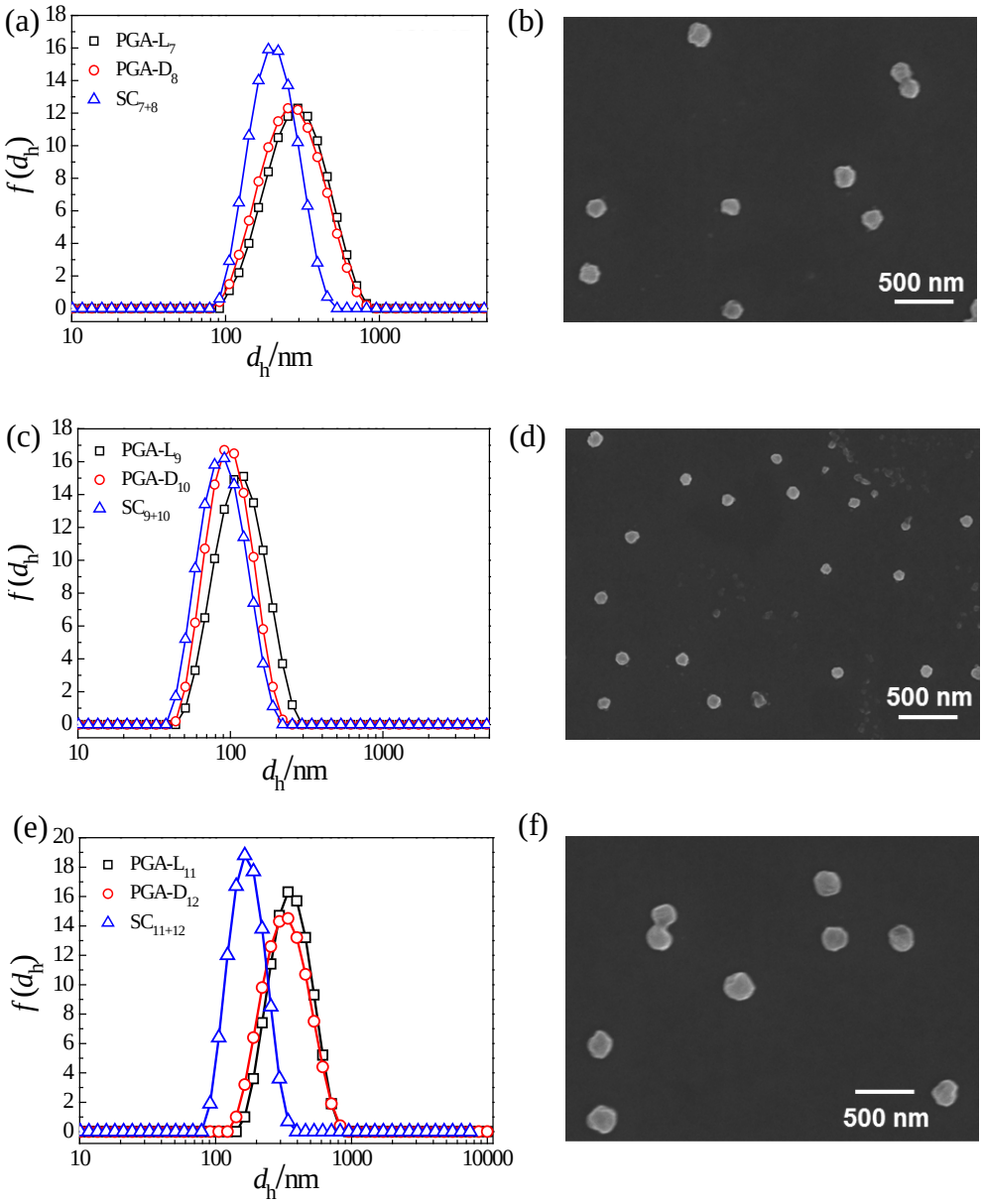

Figure 1-2. Size distribution of (a) PGA-L_7, PGA-D_8 and SC_{7+8} NPs, (c) PGA-L_9, PGA-D_{10} and SC_{9+10} NPs, and (e) PGA-L_{11}, PGA-D_{12} and SC_{11+12} NPs in PBS at the concentration of 1 mg/mL and SEM image of (b) SC_{1+2} NPs, (d) SC_{3+4} NPs, and (f) SC_{11+12} NPs

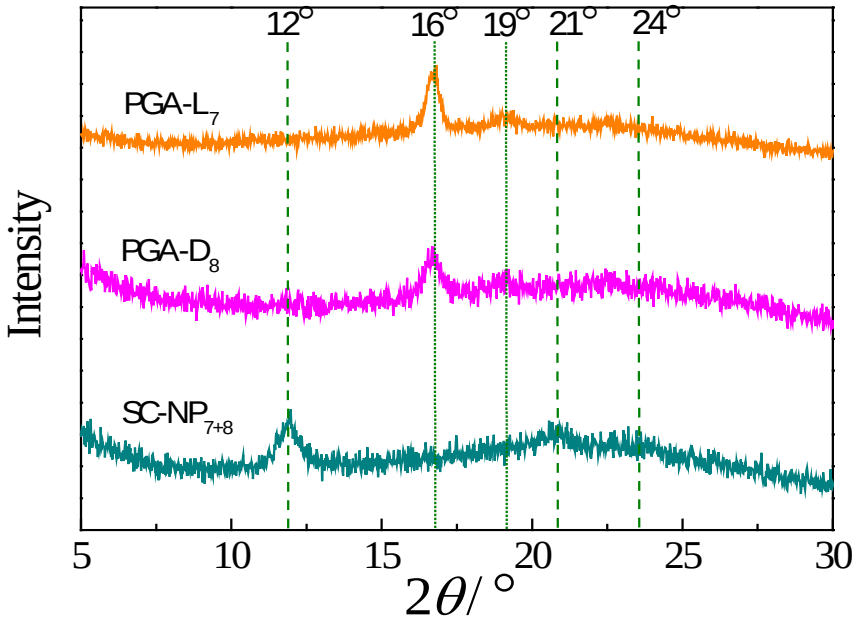

Figure 1-3. XRD patterns of PGA-L_7, PGA-D_8 NPs and stereocomplex NPs SC_{7+8}.

1.5 Conclusions

In this chapter, the amphiphilic graft copolymers, γ-PGA-*g*-PLLA and γ-PGA-*g*-PDLA, consisting of a hydrophilic backbone of γ-PGA and hydrophobic side chains of enantiomeric PLLA or PDLA, were successfully prepared. The number of enantiomeric PLA chains coupled onto γ-PGA can be controlled by changing the molar amount of PLA added into the reaction system. The effects of the molecular weight of the hydrophilic γ-PGA main chain and the grafting degree of the hydrophobic PLA side chain for the formation of NPs formed by L- or D-isomers and the equal molar mixture of the isomers in aqueous solution were investigated. These γ-PGA-*g*-PLA copolymers could form NPs, and stereocomplex crystallites were formed in the case of the mixture of γ-PGA-*g*-PLLA and γ-PGA-*g*-PDLA copolymers having a relatively large number of PLA grafts. It is expected that the stability and degradation behavior of these NPs can be regulated by controlling the crystallinity and stereocomplex formation of the core of these NPs.

References

[1]. L. Zhang, A. Eisenberg, *Science* **1995**, *268*, 1728.

[2]. A. Choucair, A. Eisenberg, *Eur. Phys. J. E* **2003**, *10*, 37.

[3]. C. Cai, J. Lin, T. Chen, X. Tian, *Langmuir* **2010**, *26*, 2791.

[4]. S. J. Holder, M. Sommerdijk, *Polym. Chem.* **2011**, *2*, 1018.

[5]. G. Gaucher, M. H. Dufresne, V. P. Sant, N. Kang, D. Maysinger, J. C. Leroux, *J. Controlled Release* **2005**, *109*, 169.

[6]. N. Nishiyama, K. Kataoka, *Adv. Polym. Sci.* **2006**, *193*, 67.

[7]. K. Letchford, H. Burt, *Eur J Pharm Biopharm*. **2007**, *65*, 259.

[8]. C. Zhang, G. Qu, Y. Sun, X. Wu, Z. Yao, Q. Guo, Q. Ding, S. Yuan, Z. Shen, Q. Ping, H. Zhou, *Biomaterials* **2008**, *29*, 1233.

[9]. X. Li, Y. Qian, T. Liu, X. Hu, G. Zhang, Y. You, S. Liu, *Biomaterials* **2011**, *32*, 6595.

[10]. *Y. H. Bae, H. Yin, J. Controlled Release **2008**, 131, 2.*

[11]. S. Chen, S. Cheng, R. Zhuo, *Macromol. Biosci.* **2011**, *5*, 576.

[12]. K. Fukushima, R. Pratt, F. Nederberg, J. Tan, Y. Yang, R. Waymouth, J. Hedrick, *Biomacromoecules* **2008**, *9*, 3051.

[13]. S. H. Kim, J. P. K. Tan, F. Nederberg, K. Fukushima, Y. Y. Yang, R. M. Waymouth, J. L. Hedrick, *Macromolecules* **2009**, *42*, 25.

[14]. J. P. K. Tan, S. H. Kim, F. Nederberg, E. A. Apple, R. M. Waymouth, Y. Zhang, J. L. Hedrick, Y. Y. Yang, *Small* **2009**, *5*, 1504.

[15]. L. Chen, Z. Xie, J. Hu, X. Chen, X. Jiang, *J. Nanoparticle Res.* **2007**, *9*, 777.

[16]. F. Nederberg, E. Apple, J. P. Tan, S. H. Kim, K. Fukushima, J. Sly, R. Miller,

R. Waymouth, Y. Y. Yang, J. L. Hedrick, *Biomacromolecules* **2009**, *10*, 1460.

[17]. T. W. Kim, T. Y. Lee, H. C. Bae, J. H. Hahm, Y. H. Kim, C. Park, T. H. Kim, M. H. Sung, H. Poo, *J Immunol* **2007**, *179*, 775.

[18]. T. Uto, T. Akagi, K. Yoshinaga, M. Toyama, M. Akashi, M. Baba, *Biomaterials* **2011**, *32*, 5206.

[19]. M. Matsusaki, K. Hiwatari, M. Higashi, T. Kaneko, M. Akashi, *Chem. Lett.* **2004**, *33*, 398.

[20]. T. Akagi, T. Kaneko, T. Kida, M. Akashi, *J. Controlled Release* **2005**, *108*, 226.

[21]. T. Akagi, X. Wang, T. Uto, M. Baba, M. Akashi, *Biomaterials* **2007**, *28*, 3427.

[22]. T. Akagi, M. Baba, M. Akashi, *Polymer* **2007**, *48*, 6729.

[23]. H. Kim, T. Akagi, M. Akashi, *Macromol. Biosci.* **2009**, *9*, 825.

[24]. T. Akagi, K. Watanabe, H. Kim, M. Akashi, *Langmuir* **2010**, *26*, 2406.

[25]. T. Akagi, T. Kaneko, T. Kida, M. Akashi, *J. Biomater. Sci. Polym. Ed.* **2006**, *17*, 875.

[26]. T. Ouchi, T. Uchida, H. Arimura, Y. Ohya, *Biomacromolecules* **2003**, *4*, 477.

[27]. H. Tsuji, F. Horii, S. H. Hyon, Y. Ikada, *Macromolecules* **1991**, *24*, 2719.

[28]. H. Tsuji, S. H. Hyon, Y. Ikada, *Macromolecules* **1991**, *24*, 5651.

Chapter 2

Characterization of γ-PGA-*g*-PLA Stereocomplex NPs and Their Potential Applications for Protein/Peptide Carriers

2.1 Summary

In chapter 1, a method to modify γ-PGA by L- or D- isomers of PLA homopolymers was reported. It is expected that the graft copolymer structure may provide for the integration of considerable functionality onto the polymer backbone that can be addressed chemically after the assembly process. In this chapter the factors that affect the formation, stability and physical state of γ-PGA-*g*-PLA NPs, such as the initial copolymers structure and NPs preparation method, were investigated. The mean diameter and degree of crystallinity of these stereocomplex NPs could be controlled by changing the grafting degree of the copolymers or the preparation methods. Moreover, the stereocomplex NPs exhibit a lower critical aggregation concentration (CAC) as well as stronger thermodynamic stability compared with the corresponding isomer NPs. It is know the hydrolytic degradation of PLA is affected by the molecular weight and crystallinity. This implies the possibility of tuning the degradation rate over a wide range of homopolymer PLA and stereocomplexed PLA composites. Expected as a potential targeting protein carrier, the surface-functionalized ability and protein encapsulation capacity of γ-PGA-*g*-PLA NPs were investigated.

2.2 Introduction

In recent years, biodegradable polymeric NPs have attracted much attention for their potential in biomedical applications. The biodegradation rate and the release kinetics of loaded drugs can be controlled by the composition ratio and the molecular weight of the polymer and graft or block co-polymers.[1]-[3] Furthermore, by modulating the polymer characteristics, one can control the release of a therapeutic agent from the NPs to achieve a desired therapeutic level in a target tissue for the required duration for optimal therapeutic efficacy. The commonly used biodegradable polymers are aliphatic polyesters, such as PLA, poly(glycolic acid) (PGA), poly(ε-caprolactone) (PCL) and their co-polymers.[4], [5] Polymeric NPs are generally formulated using the emulsion solvent evaporation method.[6] Often surfactants are used to stabilize the NPs in aqueous solution in order to prevent the aggregation and/or precipitation of water-insoluble polymers.[4] However, adequate removal of the surfactant remains a problem, and surfactant molecules are sometimes harmful in biomedical applications. Moreover, the entrapment of proteins into the NPs carrier system can be carried out through various approaches. The water-in-oil-inwater (w/o/w) double-emulsion process is popularly used to load proteins into NPs. It has a disadvantage in that these solvents have a denaturing effect on the proteins.[7],[8] In this method, the entrapped protein may be

denatured, aggregated and chemically degraded.[9],[10] Therefore, a novel type of NPs needs to be developed. Polymeric assemblies such as micelles, vesicles and NPs fabricated from amphiphilic copolymers have attracted tremendous attention in the biomedical and pharmaceutical fields for their promising applications as delivery vehicles for chemotherapeutic drugs, as well as peptides, proteins and DNAs.[11-18] In general, self-assembled amphiphilic NPs are composed of an inner hydrophobic core and an outer hydrophilic shell. The hydrophobic parts of the copolymer form the inner core of the structure, and act as a cargo incorporation site and serve as a repository, especially for hydrophobic drugs, whereas the hydrophilic shell maintains a hydration barrier that effectively protects the hydrophobic cargo.[19]-21]

However, certain issues with polymeric micelles or NPs still exist which limit their practical applications. One remaining challenge for NP-based delivery systems is the inferior *in vivo* integrity of the NPs structure and the stability as well as activity of the loaded cargos. Polymer-polymer complex formation though noncovalent interactions, including electrostatic interactions, hydrogen bonding and stereocomplexation, have been adopted as efficient strategies to enhance the stability of NPs.[22],[23] PLA, a biodegradability material widely applied in biomedical area, is a typical example used for stereocomplexation. It has been reported that PLLA/PDLA mixtures in either melt or solution states can

form stereocomplexes with distinctive physical and chemical stability due to the interactions between the L-lactyl and D-lactyl unit sequences.[24],[25] Application of this interaction was first employed in micelle stabilization by Leroux's group with stereocomplex block copolymer micelles obtained through the self-assembly of equimolar mixtures of poly(ethylene glycol)-*block*-poly(L-lactide) and poly(ethylene glycol)-*block*-poly(D-lactide) in water. These sterocomplex micelles possessed partially crystallized cores and exhibited kinetic stability superior to micelles prepared with isotactic or racemic polymers alone.[26] Furthermore, Nagahama *et al.* also reported the preparation of stereocomplex nanogels through the self-assembly of dextran-*graft*-poly(L-lactide) (Dex-*g*-PLLA) and dextran-*graft*-poly(D-lactide) (Dex-*g*-PDLA) graft copolymers and proved that the kinetic stability of nanogels can be enhanced.[27] However, the majority of research performed on the formation of NPs through PLA stereocomplexation is based on copolymers lack of functional groups and among them few studies have focused on their application as protein/peptide delivery system.

In chapter 1, a method to modify γ-PGA by L- or D- isomers of PLA homopolymers and γ-PGA-*graft*-PLA copolymers with different grafting degree was developped.[28] It is expected that the graft copolymer structure may provide for the integration of considerable functionality onto the polymer backbone that

can be addressed chemically after the assembly process. Furthermore, as we know the hydrolytic degradation of PLA is affected by various factors such as the chemical configuration, molecular weight, crystallinity, and environmental conditions. This implies the possibility of tuning the degradation rate over a wide range of homopolymer PLA and stereocomplexed PLA composites. However, it is known that the inherent physical structure and chemical properties of NPs including size, morphology, surface characteristics, and the hydrophobic-hydrophilic balance of the copolymers can dictate a NP's degradation behavior and cargo loading efficiency as a delivery vehicle. Therefore, in this chapter, the factors that affect the formation, stability and physical state of γ-PGA-*g*-PLA NPs, such as the initial copolymers structure and NPs preparation method, were investigated by employing a series of amphiphilic enantiomeric γ-PGA-*g*-PLA copolymers with different γ-PGA molecular weights and PLA grafting degrees to prepare isomeric and stereocomplex NPs. Furthermore, expected as a potential targeting protein carrier, the surface-functionalized ability and protein encapsulation capacity of γ-PGA-*g*-PLA NPs were investigated by using ovalbumin (OVA) and 9-mer WT1 peptide.

2.3 Experimental Section

Materials

L-lactide and D-lactide were purchased from Purac Biochem BV (Gorinchem, the Netherlands) and were re-crystallized twice from ethyl acetate prior to use. Poly(γ-glutamic acid) (γ-PGA, number average molecular weight, M_n = 75 kDa, molecular weight distribution, M_w/M_n = 2.0), stannous octanoate [$Sn(Oct)_2$], OVA and other chemicals were purchased from Wako Pure Chemical Industries (Tokyo, Japan). Anhydrous toluene, anhydrous dimethyl sulfoxide (DMSO) and anhydrous 1,4-dioxane used as reaction solvent were purchased from Wako Pure Chemical Industries (Tokyo, Japan), and were used without further purification. EDC and DMAP were purchased from Sigma (St. Louis, MO), and were used as received. The WT1 peptide (RMFPNAPYL) was purchased from Scrum Japan Ltd (Osaka, Japan).

Synthesis of γ-PGA-g-PLA amphiphilic graft copolymer

Briefly, the γ-PGA-*g*-PLLA and γ-PGA-*g*-PDLA graft copolymers were synthesized by a coupling reaction. γ-PGA (100 mg, 0.775 unit mmol), stoichiometric amounts of EDC (149 mg, 0.775 mmol) and DMAP (95 mg, 0.775 mmol) were dissolved in 10 mL of dehydrated DMSO. Then 1 mL of pre-dissolved PLLA or PDLA/dioxane solution at various concentrations was

slowly added into the mixture solution under nitrogen protection. The reaction was allowed to continue for 24 h at 40°C with stirring. The reaction mixture was dialyzed against pure water using a dialysis membrane (molecular weight cut-off 50 kDa) for two days, and lyophilized until dry. The obtained products were washed twice by an excess amount of THF to remove the uncoupled PLLA or PDLA. The obtained precipitate was then collected by centrifugation, and dried under vacuum overnight. The average number of PLLA or PDLA grafted per γ-PGA chain was determined by ^{1}H NMR analysis in DMSO-d_6 using the integrals of the methylene peaks (2.20 ppm, NHCHCH_2CH$_2$ and 1.74-1.90 ppm, NHCHCH$_2$CH_2) in the γ-PGA backbone and the methine peaks (5.20 ppm, CHCH$_3$ of PLA) in the PLA main chain as shown in Figure 2-1. The copolymers used in this chapter are listed in Table 2-1.

Table 2-1. Synthesis of γ-PGA-*g*-PLLA and γ-PGA-*g*-PDLA copolymers

Code	Sample	M_w of γ-PGA (kDa)	M_w of PLA (kDa)	Feed Ratio[a]	Yield (%)[b]	Grafting Degree (%)[c]	PLA Content (wt.%)[d]
PGA-L_7	γ-PGA_{75k}-*g*-$PLLA_{2.6}$	75	2.6	2	56	2.6	34
PGA-D_8	γ-PGA_{75k}-*g*-$PDLA_{2.2}$	75	2.5	2	52	2.2	30
PGA-L_9	γ-PGA_{10k}-*g*-$PLLA_{3.4}$	10	2.6	2	53	3.4	41
PGA-D_{10}	γ-PGA_{10k}-*g*-$PDLA_{3.1}$	10	2.5	2	57	3.1	38
PGA-L_{11}	γ-PGA_{10k}-*g*-$PLLA_{7.4}$	10	2.6	3	26	7.4	60
PGA-D_{12}	γ-PGA_{10k}-*g*-$PDLA_{6.1}$	10	2.5	3	28	6.1	55

[a] Feed ratio = PLA/γ-PGA (g/g);

[b] Yield = [(γ-PGA-*g*-PLA) / (PLA + γ-PGA)] × 100% (g/g);

[c] Grafting degree and number of grafted PLA chains were estimated by ^{1}H NMR (solvent DMSO-d_6);

[d] PLA content was the content of PLA unit in wt. % = [(M_w of PLA × the number of grafted PLAs) / (M_w of γ-PGA-*g*-PLA copolymers)].

Preparation of γ-PGA-g-PLA NPs

Aqueous copolymer NPs were prepared by the dialysis method. Briefly, γ-PGA-*g*-PLLA, γ-PGA-*g*-PDLA and an equal molar mixture of PLLA and PDLA copolymer were first dissolved in DMSO, a solvent for both γ-PGA and PLA, to a concentration of 10 mg/mL. Then, phosphate buffer saline (PBS; 10 mM, pH 7.4, 0.15 M NaCl), which is a non-solvent of PLA, was added dropwise into the copolymer solution with vigorous stirring until the water content reached 50 vol. %. The solutions were transferred into a dialysis tube (MWCO: 1,000 Da) for dialysis against pure water to remove the DMSO. After dialysis, the particle size and distribution were measured by dynamic light scattering (DLS).

Steady-state fluorescence spectroscopy

The steady-state fluorescence spectra of γ-PGA-*g*-PLLA, γ-PGA-*g*-PDLA and an equal molar mixture of the two in aqueous media were recorded on a JASCO FP-600 spectrofluorometer at room temperature using pyrene as a hydrophobic probe. Sample solutions were prepared by adding known amounts of pyrene in acetone to each of a series of glass vials. The amount of pyrene was chosen so as to give a final pyrene concentration of 1×10^{-6} M. After evaporation of the acetone by flushing with gaseous nitrogen, solutions of the copolymers at various concentrations in PBS were added to the probe. The samples were equilibrated after incubation overnight at room temperature. The fluorescence emission

spectra of pyrene then were measured at λ_{ex} 339 nm, and for excitation, the λ_{em} was 372 nm.

Preparation of stereocomplex NPs in acetonitrile

The solubility of all γ-PGA-*g*-PLA samples in acetonitrile were studied by the dissolving copolymers in acetonitrile at a concentration of 2 mg/mL with stirring at 60°C overnight. The soluble copolymers PGA-L_{11} (γ-PGA_{10k}-*g*-$PLLA_{7.4}$) and PGA-D_{12} (γ-PGA_{10k}-*g*-$PDLA_{6.1}$) were then dissolved in acetonitrile at a concentration of 10 mg/mL. The solutions were stirred at 60°C for 72 h for complete dissolution. After dissolving, the same volume of an acetonitrile solution of PGA-L_{11} and PGA-D_{12} copolymers was mixed together and stirred at room temperature until the solution became turbid. The stereocomplex NPs were collected by centrifugation at 14,500 rpm for 20 minutes and then redisposed in PBS to measure the particle size and distribution by DLS. The samples for XRD measurement were prepared by lyophilization.

Kinetic stability analysis of γ-PGA-g-PLA NPs

The kinetic stability of NPs composed of enantiomeric γ-PGA-*g*-PLA copolymers and an equimolar mixture of two was investigated by DLS in the presence of the destabilizing agent sodium dodecyl sulfonate (SDS). PBS solutions of the NPs at 3.3 mg/mL were mixed with a 2% SDS solution (20

mg/mL) at a volume ratio of 2:1 (SDS final concentration 6.7 mg/mL). The mixed solutions were then incubated at 37°C. After 2, 4, 6, 8, 10, 12, 24 and 48 hours, DLS measurements of the mixed solutions were carried out.

Immobilization of OVA or WT1 onto γ-PGA-g-PLA NPs

To prepare the protein/peptide immobilized γ-PGA-*g*-PLA NPs, the carboxyl groups of the NPs (10 mg/ml in PBS) was first activated by EDC (1 mg/ml in PBS) for 20 min. And then, the NPs (5 mg) obtained by centrifugation (14500 rpm for 10 min) were dispersed in 1 ml of OVA or WT1 peptide solution at various concentration (0.5, 1 and 2 mg/ml in PBS), and the mixture was incubated at 4°C for 24 h. After the reaction was terminated, the NPs were isolated by centrifugation, washed twice by PBS, and resuspended at in PBS at the concentration of 10 mg/ml. The amount of proteins covalently immobilized onto the NPs was calculated from the amount of non-loaded proteins remaining in the suspending medium by the Lowry method [29] and the results are presented as means ± SD values (n=3). The loading efficiency was calculated as (the immobilized and encapsulated protein amount onto the NPs / initial feeding amount of proteins) × 100%.

Preparation of OVA encapsulated γ-PGA-g-PLA NPs

To prepare the OVA-encapsulated γ-PGA-*g*-PLA NPs, 0.5-2 mg of OVA was

dissolved in 1 ml of PBS and slowly added into 1 ml of the DMSO solution of γ-PGA-*g*-PLA isomers or mixture of two (10 mg/ml) with stirring. The resulting solution was centrifuged at 15,000 rpm for 10 min and repeatedly rinsed by PBS twice, and resuspended at in PBS at the concentration of 10 mg/ml. The OVA loading content was measured by the Lowry method, as described above and the results are presented as means ± SD values (n=3). The loading efficiency was calculated as (the immobilized protein amount onto the NPs / initial feeding amount of proteins) × 100%.

Characterization

DLS measurements were performed on a Zetasizer Nano ZS (Malvern Instruments, UK) with a He-Ne laser (λ_0 = 633 nm) as the light source. All data were averaged over three measurements at a concentration of 1 mg/ml in PBS. The surface charge of the NPs was determined by zeta potential measurements using a Zetasizer Nano ZS. All data were averaged over three measurements, and the NPs suspension at a concentration of 0.1 mg/ml in PBS was used for zeta potential measurements. The morphology of the NPs was observed by scanning electron microscopy (SEM) (JSM-6700F, JEOL) at 10 kV. A drop of the NPs suspension was deposited onto a glass surface, which was fixed on metallic supports with carbon tape. After drying, the samples were coated with osmic acid. The XRD patterns were recorded on a RIGAKU RINT2000 instrument with a Cu

K α (λ = 0.154 nm) source at room temperature, operated at 40 kV and 200 mA with a Ni filter and the XRD spectra were analyzed using the MDI Jade 5.0 software. The samples were examined at 2θ equal to 5-30°. The patterns were then curve-resolved into amorphous hollow and crystalline reflection peaks. The main reflection peaks were integrated and used to calculate the crystalline index (*CI* %) of the samples.

2.4 Results and Discussion

Critical Aggregation Concentration (CAC) of γ-PGA-g-PLA Copolymers

In order to demonstrate the formation of NPs and to study the self-assembly behavior of γ-PGA-*g*-PLA copolymers in PBS, the fluorescence spectra of γ-PGA-*g*-PLLA, γ-PGA-*g*-PDLA and the equimolar mixture of the two were measured by steady-state fluorescence spectroscopy with pyrene as a probe. It is well-established that in the presence of NPs and other similar aggregations, pyrene is solubilized into the hydrophobic domains.[30],[31] As a result, significant changes in the spectroscopic properties were observed consistent with the decrease in the polarity of the environment for the probe.[32] The emission spectra of pyrene (1×10^{-6} M) dissolved in the PBS solution of γ-PGA-*g*-PLA copolymers at various concentrations were measured. Upon increasing copolymer concentration, the fluorescence maximum-intensity at 372 nm (I_1) increased and the intensity of vibrational band one to vibrational band three

(I_1/I_3) decreased, indicating that the PLA chains grafted on the γ-PGA main chain started to associate with each other through hydrophobic interactions in PBS, and the probe started to transfer from an aqueous solution to a non-polar environment. Noda *et al.* reported that the CAC value of a polymer aggregate consisting of hydrophobic domains surrounded by charged segments can be calculated from the steady-state fluorescence excitation spectra of pyrene probes.[31] To study the CAC of the γ-PGA-*g*-PLA NPs, the excitation spectra of pyrene were also measured in the presence of copolymers at various concentrations. The spectra of an equimolar mixture of PGA-L_{11} and PGA-D_{12} in PBS at various concentrations are shown in Figure 2-1a. As shown in these spectra, the peaks associated with the (0,0) band of pyrene at 333 nm in a low polymer concentration shifted to 337 nm at higher concentrations. This red shift of the excitation spectra is characterized by a change in the I_{337}/I_{333} intensity ratio as a function of the logarithm of the copolymer concentration (Figure 2-1b-d). It is clear that the I_{337}/I_{333} values remained relatively constant below a certain concentration, and then changed substantially, reflecting the partitioning of the pyrene into the more hydrophobic environment. The CAC value was obtained from the intersection point of the baseline and the tangent of the rising I_{337}/I_{333} values. The CAC values of γ-PGA-*g*-PLA copolymers with different compositions are listed in Table 2-2. All copolymers exhibited a relatively low CAC value, which decreased with an

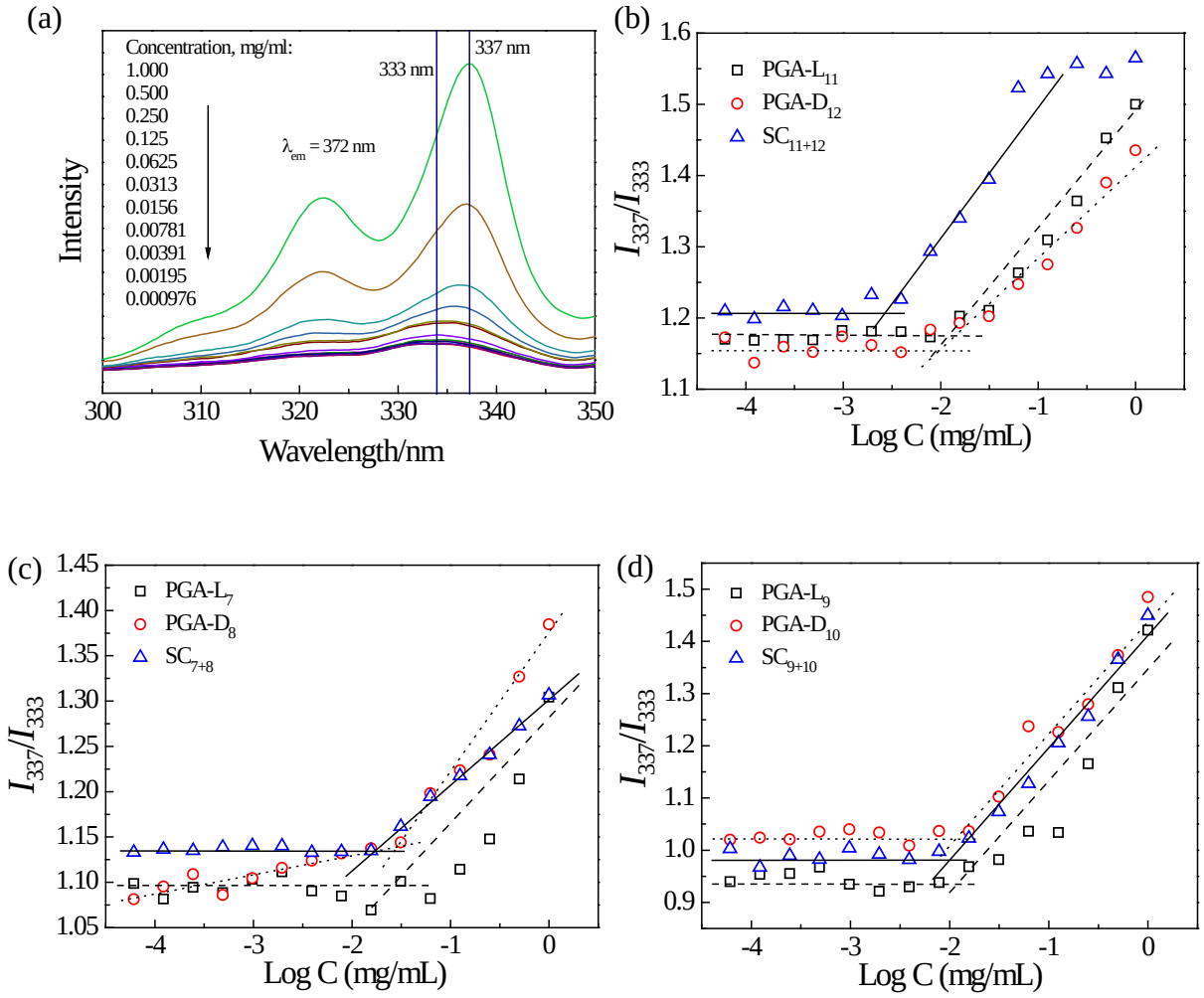

Figure 2-1. (a) Fluorescence excitation spectra of pyrene in PBS in the presence of SC_{5+6} NPs at different concentrations. Change in the fluorescence intensity ratio (I_{337}/I_{333}) versus the concentration of (b) PGA-L_{11}, PGA-D_{12} and SC_{11+12} NPs, (c) PGA-L_7, PGA-D_8 and SC_{7+8} NPs, and (d) PGA-L_9, PGA-D_{10} and SC_{9+10} NPs.

increase in the PLA content. These results were consistent with previous studies on stereocomplex micelles formed by PEG-*b*-PLA[26] and stereocomplex nanogels formed by Dex-*g*-PLA[27], which indicated that in aqueous solution, the self-assembly of γ-PGA-*g*-PLA is driven by hydrophobic interactions between the PLA chains. Furthermore, all stereocomplex NPs exhibited lower CAC values than NPs formed by isomers, especially SC_{11+12}. The lower CAC values implied that the mixture of enantiomeric copolymers has a strong tendency to form NPs, and that the cores of the stereocomplex NPs were stabilized by strong van der Waals interactions.[33]

Table 2-2. Characterization of NPs formed by individual and mixed γ-PGA-*g*-PLA copolymers.

Sample	Particle		Zeta Potential[a] (mV)	CAC[c] (mg/mL)	Crystalline index[e] (*CI* %)
	d_h [a] (nm)	PDI[b]			
PGA-L_7	260 ± 7.1	0.14 ± 0.01	-18.3 ± 0.3	0.032	11.9
PGA-D_8	245 ± 7.2	0.20 ± 0.02	-19.5 ± 0.3	0.039	10.8
[d]SC_{7+8}	190 ± 0.8	0.12 ± 0.04	-20.6 ± 1.3	0.025	26.2
PGA-L_9	110 ± 4.4	0.12 ± 0.02	-25.6 ± 1.8	0.012	27.3
PGA-D_{10}	95 ± 2.9	0.13 ± 0.01	-24.1 ± 1.4	0.010	20.6
[d]SC_{9+10}	90 ± 0.5	0.10 ± 0.01	-26.3 ± 1.5	0.007	38.6
PGA-L_{11}	330 ± 2.0	0.09 ± 0.01	-26.9 ± 0.8	0.013	46.2
PGA-D_{12}	300 ± 3.2	0.11 ± 0.03	-28.1 ± 1.7	0.016	40.1
[d]SC_{11+12}	210 ± 1.7	0.07 ± 0.03	-29.0 ± 1.1	0.002	57.8

[a] The particle size and zeta potential of individual and stereocomplex γ-PGA-*g*-PLA NPs were measured in PBS at 1 mg/mL (mean ± SD of three independent experiments is shown);

[b] Polydispersity index;

[c] Critical aggrigation concentration (CAC) was estimated by the fluorescence spectroscopy using pyrene as probe;

[d] SC means stereocomplex formed by the equal molar mixture of PGA-L and PGA-D, e.g. SC_{1+2} means stereocmplex NPs formed by the mixture of PGA-L_1+PGA-D_2 et cetera;

[e] The crystalline index (*CI* %) was calculated from XRD spectra by the MDI Jade 5.0 software.

Wide angle X-ray diffraction patterns of γ-PGA-g-PLA NPs

In order to further study the physical state of the γ-PGA-*g*-PLA copolymer NP cores, XRD measurements were carried out on lyophilized NPs. The XRD patterns of NPs formed by L- or D- isomers alone and the enantiomeric mixtures are shown in Figure 2-2. Enantiomeric PLLA and PDLA homopolymers are both crystallizable in an orthorhombic or pseudo-orthorhombic unit cell with a 10_3 helical conformation (α-form).[34] In the case of NPs prepared by L-isomers, the α-form homocrystal peaks of PDLA at the 2θ values of 16° and 19° was detected in all samples. Characteristic peaks of the PLA stereocomplex crystalline structure at the 2θ values of 12°, 21° and 24° were observed in all NPs fabricated from equimolar mixtures of enantiomeric copolymers (Figure 2-2b). The *CI* % of PLA isomers and stereocomplex calculated by the MDI Jade 5.0 software from the XRD spectra are listed in Table 2-2. In all samples, the sterocomplex NPs (SC_{7+8}, SC_{9+10} and SC_{11+12}) containting equimolar amount of γ-PGA-*g*-PLLA and γ-PGA-*g*-PDLA displayed the higher crystallinity than NPs prepared from isomers alone. The stereocomplex crystallinity gradually increased from 26 to 58% with an increase in the PLA content (wt%) in the graft coplymer. It is reported that in the case of micelles obtained through the self-assembly of PEG-*b*-PLLA, PEG-*b*-PDLA and equimolar mixtures of the two in water, the stereocomplex micelles were characterized by a higher aggregation number

(N_{agg}) than micelles obtained from isomers alone.[26] Therefore, in the case of γ-PGA-*g*-PLA stereocomplex NPs, due to the increased number of copolymer chains involved in the self-assembling process and the strong van der Waals interactions between the two isomers, the PLA crystallites in stereocomplex NP cores adopt a more compact conformation, allowing higher crystallinity. Moreover, the crystallinity of both α-form homocrystals and stereocomplex crystals were increased by changing the main chain length or by increasing the grafting degree, which suggested that the crystallinity of the NPs could be controllable.

Kinetic stability analysis of γ-PGA-g-PLA NPs

The kinetic stability of the isomeric and stereocomplex γ-PGA-*g*-PLA NPs was studied by DLS in the presence of SDS, which acts as a destabilizing agent. Figure 2-3 shows the time dependence of the DLS intensity of the NPs formed by PGA-L_{11}, PGA-D_{12} and an equal molar mixture of two. SDS-treated PGA-L_{11} and PGA-D_{12} NPs exhibited a decrease in scattered light intensity within the first 10 h. The signal then remained at about 60% of the initial signal intensity, suggesting the dissociation of a certain fraction of NPs. In contrast, the stereocomplex NPs were more stable because they showed only a minimal decrease in scattered light intensity. Even after 48 h, the d_h retained more than 90% of their initial signal intensity, indicating strong kinetic stability in aqueous

solution. In fact, several studies have shown that the kinetic stability of micelles can be improved by PLA stereocomplexation. Leroux *et al.*[26] reported that the R_h of SDS-treated PEG-*b*-PDLLA micelles (amorphous core) exhibited a drastic decrease within 2 h, and that the scattered light intensity remained low (50%). In contrast, the stereocomplex micelle solutions were substantially more stable as they showed only a minimal decrease in scattered light intensity and the solutions retained more than 80% of their initial signal intensity even after 4 days. Nagahama *et al.*[27] also reported that stereocomplex nanogels prepared by the mixture of Dex-*g*-PLA isomers showed higher stability compared with nanogels with amorphous PLA cores. The results obtained here support the previous studies, suggesting that the physical properties of the NP cores could be an important factor to control NP stability. Furthermore, the stability of isomeric and stereocomplex γ-PGA-*g*-PLA NPs in various buffer solutions with different pH values from 5 to 10 were also studied. The isomeric and stereocomplex NPs were stable over the pH range of 5 to 8 for over 2 weeks. On the other hand, degradation or dissociation of NPs occurred in a pH-dependent manner over the pH range of 9 to 10, which due to the increased solubility of γ-PGA and the hydrolysis of PLA in alkaline condition .

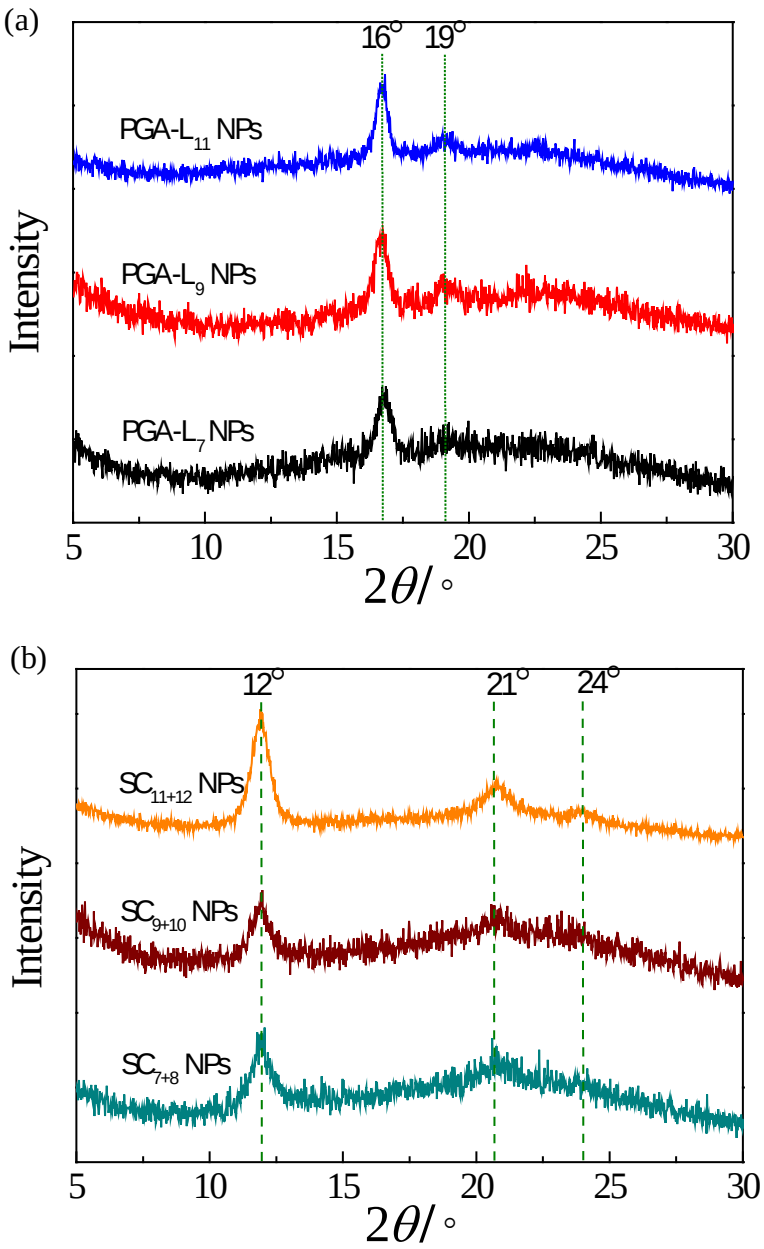

Figure 2-2. XRD patterns of (a) NPs formed by PGA-L_7, PGA-L_9 and PGA-L_{11} copolymers, and (b) stereocomplex NPs SC_{7+8}, SC_{9+10} and SC_{11+12}.

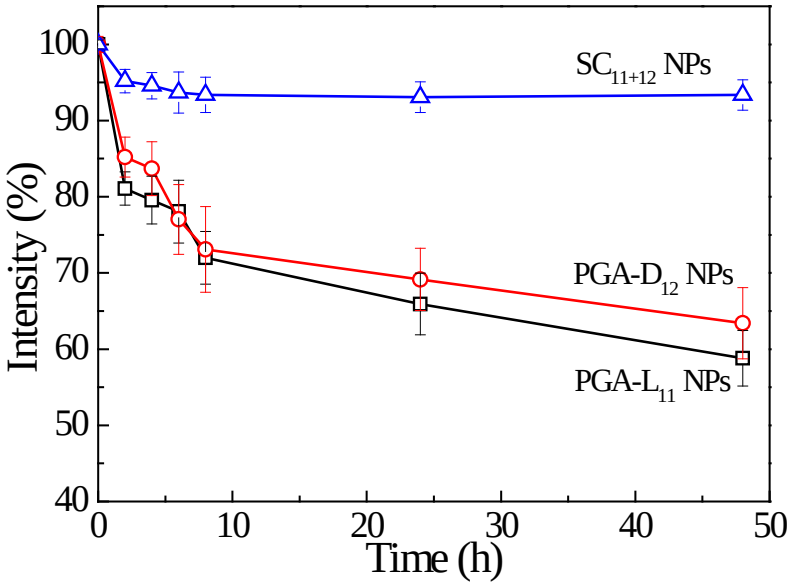

Figure 2-3. DLS intensities of PGA-L_{11}, PGA-D_{12}, and SC_{11+12} NPs versus time after the addition of SDS (6.7 mg/mL final concentration). The results are presented as means ± SD values (n=3).

Characterization of stereocomplex NPs formed in acetonitrile

In order to further study the crystallinity of the NP cores formed by the stereocomplexation of enantiomeric γ-PGA-*g*-PLA copolymers, acetonitrile, a strongly complexing solvent for enantiomeric PLA, was used for NPs preparation. Tsuji *et al.* reported that the racemic crystallization of PLLA and PDLA mixtures takes place in acetonitrile, even when the solution concentration is as low as 10 mg/mL, whereas solutions of a single polymer, either PLLA or PDLA, remained homogeneous at the same concentration.[35] Since acetonitrile is a nonsolvent for γ-PGA, the solubility of all γ-PGA-*g*-PLA samples in acetonitrile were studied. In all samples, only PGA-L_{11} and PGA-D_{12} were soluble in acetonitrile at 60°C, and the change in solubility was due to the high PLA content (over 50%). After dissolution, the same volume of acetonitrile solutions of PGA-L_{11} and PGA-D_{12} copolymers were mixed together at room temperature with vigorous stirring. During stirring, the racemic mixture of PGA-L_{11} and PGA-D_{12} formed the stereocomplex of PLLA and PDLA by the alternate packing of β-form 3_1 helices of the opposite absolute configuration (left- versus right-handed, respectively) side by side with van der Waals contacts [36] and the solution then became turbid, indicating the formation of NPs (SC_{11+12}-AcN). The size and morphology of the SC_{11+12}-AcN NPs in aqueous medium were characterized by DLS and SEM. DLS experiments were performed on a PBS solution of SC_{11+12}-AcN NPs at varying

concentrations from 0.1 to 5.0 mg/mL. The SC_{11+12}-AcN NPs exhibited nanoscale size and monodispersity. As shown in Figure 2-4a, the d_h of the SC_{11+12}-AcN NPs in PBS at various concentrations remained almost constant (330-340 nm) with narrow polydispersity, which indicated the high stability of SC_{11+12}-AcN NPs. When compared with SC_{11+12} NPs prepared by the dialysis method (240 nm), the size of the SC_{11+12}-AcN NPs was much bigger. This is might be due to that the PLLA and PDLA side chains on the copolymers preferred to undergo the racemic crystallization process in acetonitrile, and that the number of polymer chains associated during the self-assembly process were increasing. A SEM image of the SC_{11+12}-AcN NPs is shown in Figure 2-4b. It is clear that the NPs most often had a spherical shape, and a size close to that measured by DLS.

The physical structure of the core of the stereocomplex NPs prepared in acetonitrile was studied by XRD measurements. As shown in Figure 2-5a, crystalline peaks at 2θ values of 12°, 21° and 24° were clearly detected, and confirmed the crystalline structure of the stereocomplexed PLA in the core of the NPs. Furthermore, compared with stereocomplex NPs formed by the dialysis method (*CI* % = 57.8%), the crystallinity of stereocomplex NPs form in acetonitrile was about 75%, thus implying the bigger size of the crystalline domains and a denser polymeric packing. These results revealed that the

crystallinity of the NP core could also be controlled by using different preparation methods and initial solvents.

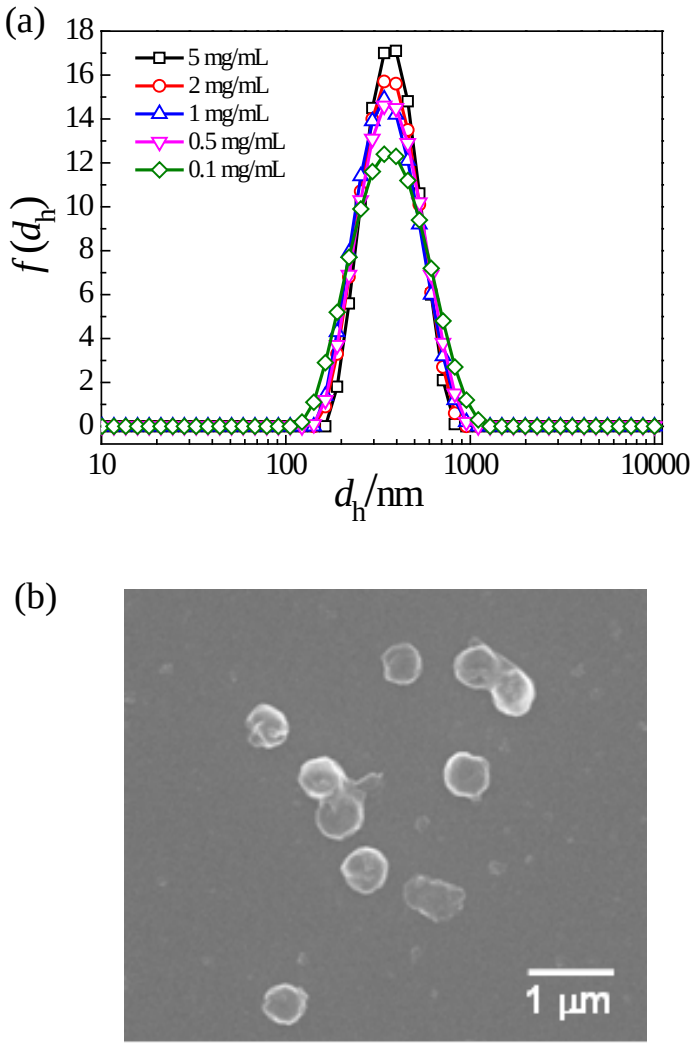

Figure 2-4. (a) Size distribution of SC_{11+12}-AcN NPs in PBS at concentrations of 0.1 g/L (d_h = 333 nm), 0.5 g/L (d_h = 334 nm), 1.0 g/L (d_h = 335 nm), 2.0 g/L (d_h = 334 nm), and 5.0 g/L (d_h = 344 nm). (b) SEM image of SC_{11+12}- NPs.

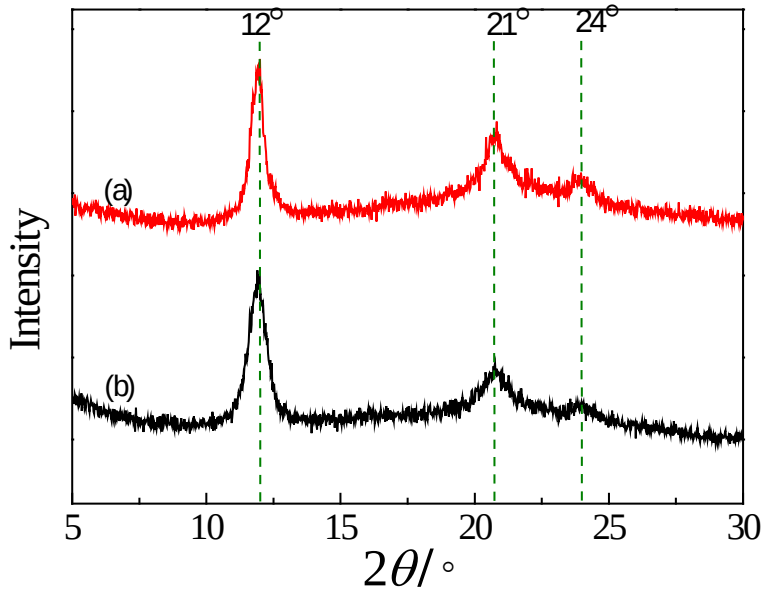

Figure 2-5. XRD patterns of stereocomplex NPs from an equimolar mixture of PGA-L_{11} and PGA-L_{12} copolymers prepared (a) in acetonitrile, and (b) by the dialysis method.

Surface immobilization of protein/peptide onto γ-PGA-g-PLA NPs

For targeted drug delivery, biorecognition elements often need to be immobilized on the NP surfaces. Due to the low hydrophobic substitution degree, NPs consisting of γ-PGA-*g*-PLA have a large amount of carboxyl group on/in them. Thus, they should be potentially applicable for the immobilization of bioactive agents, such as proteins, peptides, targeting ligands and cationic molecules. In order to explore the feasibility of protein/peptide immobilization on γ-PGA-*g*-PLA NPs, OVA and WT1 peptide was used as a model for this study. The immobilization of OVA and WT1 peptide onto the NPs formed by L- or D- isomers and the equal mixture of two were successfully achieved by forming amide bond between the amide group of OVA/WT1 peptide and the carboxyl group on surface of the γ-PGA-*g*-PLA NPs. As compared to untreated NPs, the protein-immobilized NPs did not change their particle size. Figure 2-6 shows the effects of the protein concentration on the amount of protein immobilized onto the NPs and the results indicated that the amount of OVA and WT1 peptide covalently immobilized increased upon increasing the initial feeding amount. These results demonstrated that the immobilization of protein onto the surface of nanoparticles was possible via covalent bonding. The loading efficiencies of WT1 peptide in both L- or D-isomer NPs and stereocomplex NPs reached about 50 wt.% at 2 mg/mL peptide concentration, which are higher than

that of OVA (30 wt.%) under the same conditions. The differences may be attributed to the size, molecular weight and number of amino groups on the surface of the proteins. In a previous study of our group, OVA-surface immobilized NPs formed from γ-PGA-Phe copolymer with 53% grafting degree were prepared in order to study their potential application as protein carriers. The loading efficiency of OVA immobilization onto the surface of the γ-PGA-Phe NPs was only about 5 wt.%. However, in the case of γ-PGA-*g*-PLA NPs with the similar hydrophobic content (PGA-L_{11} NPs, PGA-D_{12} NPs and SC_{11+12} NPs), due to low substitution degree and higher carboxyl group density, the protein/peptide immobilization efficiency was enhanced significantly .

Encapsulation of protein into γ-PGA-g-PLA NPs

Besides surface immobilization, protein encapsulation of the γ-PGA-*g*-PLA isomeric or stereocomplex NPs was investigated to evaluate the potential applications as protein carriers. The encapsulation of OVA into the γ-PGA-*g*-PLA NPs was successfully achieved. Similarly tendency as surface immobilization, the amount of OVA encapsulated into the NPs was increased upon increasing the initial feeding amount of OVA (Figure 2-7a). In the case of the encapsulation method, the OVA loading efficiency reached about 50 wt.% at 0.5 mg/ml of OVA and was obviously increased with an increase in the initial

OVA concentration in all isomeric and stereocomplex γ-PGA-*g*-PLA NPs. When the OVA concentration reached 2mg/mL, the loading efficiencies of OVA both

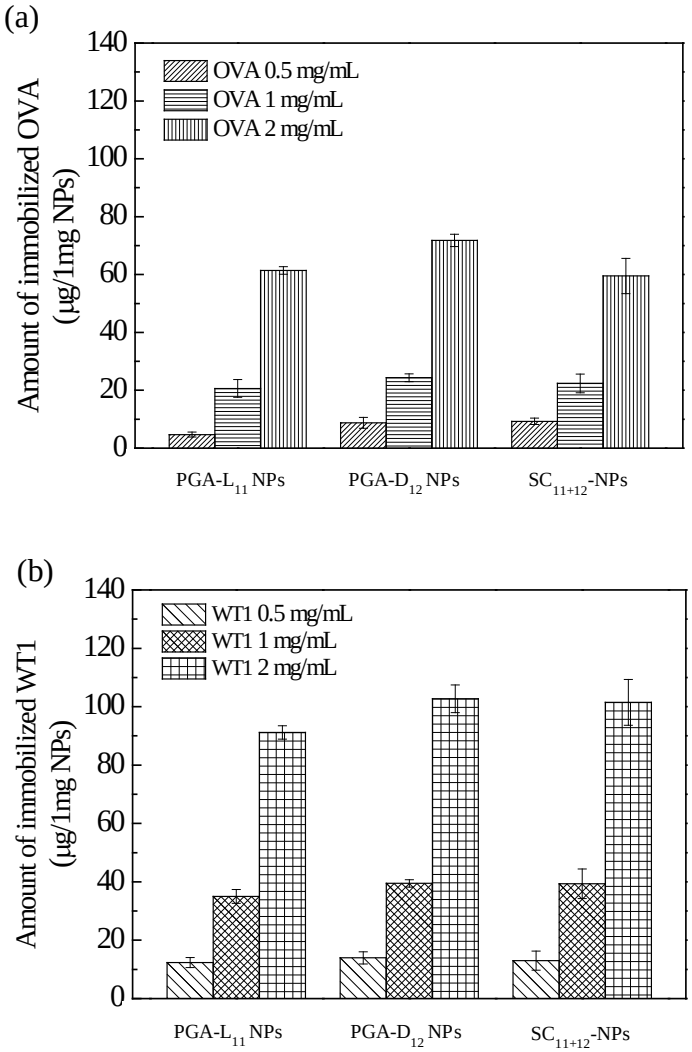

Figure 2-6. Effect of the protein concentrations on the amount of (a) OVA, and (b) WT1 peptide immobilized onto PGA-L_{11}, PGA-D_{12} and SC_{11+12} NPs. The amount of protein loaded was calculated by the immobilized amount of protein (mg) / NP weight (1 mg). The results are presented as means ± SD values (n=3).

L- or D-isomer NPs and stereocomplex NPs reached up to about 70 wt.%, which indicated that the inner space of γ-PGA-*g*-PLA isomeric stereocomplex NPs have great potential for OVA loading. From the DLS measurements, the d_h of the unloaded γ-PGA-*g*-PLA NPs were 330 nm for PGA-L_5, 300 nm for PGA-D_6 and 210 nm for SC_{5+6}, with a monodispersed distribution. The particle size of the NPs was greatly increased when the OVA was encapsulated. Figure 2-7 shows that the size of the γ-PGA-*g*-PLA NPs increased depending on the amount of OVA loaded into the NPs, which might due to an increase in swelling capacity due to the hydrophilic properties of OVA or electrostatic repulsion between γ-PGA and OVA with the same anionic charge. Furthermore, the encapsulated OVA were stable and not released from the NPs over weeks in neutral buffer, which suggest that the OVA is stable encapsulated into the NPs.

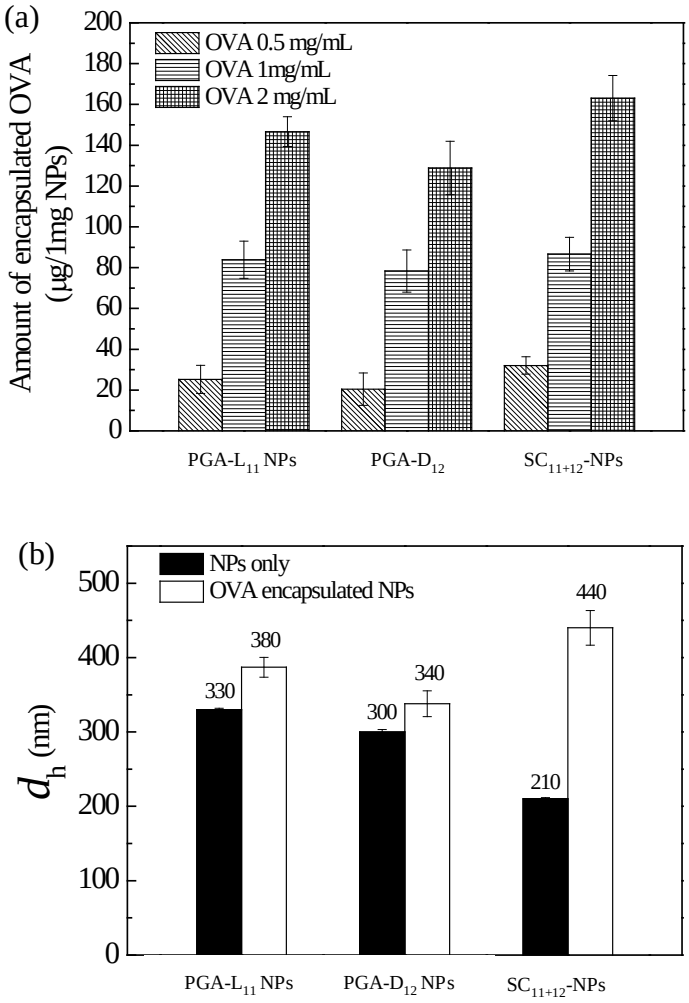

Figure 2-7. (a) Effect of the protein concentrations on the amount of OVA encapsulated into PGA-L_{11}, PGA-D_{12} and SC_{11+12} NPs. The amount of protein loaded was calculated by the immobilized amount of protein (mg) / NP weight (1 mg). (b) Changes in the size of the OVA encapsulated NPs measured in PBS by DLS. The results are presented as means ± SD values (n=3).

2.5 Conclusion

In conclusion, the effects of the molecular weight of the hydrophilic γ-PGA main chain and the grafting degree of the hydrophobic PLA side chain for the formation, stability and crystallinity of NPs formed by L- or D-isomers and the equal molar mixture of the isomers in aqueous solution were investigated. As a key factor, the hydrophobic/hydrophilic balance plays an important role in controlling the size, self-assembly behavior, physical state and stability of γ-PGA-*g*-PLA isomeric and sterocomplex NPs. Furthermore, besides hydrophobic content, the crystallinity of sterocomplex NPs can also be enhanced by using different preparation method. It is shown that stereocomplex NPs formed from acetonitrile have a higher crystallinity. Expected as a potential delivery system, the encapsulation of model protein OVA into both the γ-PGA-*g*-PLA isomeric NPs and stereocomplex NPs were successfully achieved. Moreover, due to the large number of carboxyl groups on the γ-PGA-*g*-PLA NPs, bioactive agents such as proteins and peptides and other functional moieties are able to immobilize on the surface of NPs. Therefore, the obtained surface functionalized protein loaded NPs are expected to apply as specific targeting nanocarries for drug, protein delivery and immunotherapy. Once located at the target site, the NPs should then degradation and release their content. The release kinetics may be influenced by the stereocomplex formation and crystallinity of

the core of NPs. It is proposed that such polymeric systems may be useful for targeted NP-based drug delivery. Further studies including the protein releasing behavior and their applications as protein delivery carriers for immunotherapy *in vitro* and *in vivo* are now in progress.

Reference

[1] D. T. O'Hagan, H. Jeffery, S. S. Davis, *Int. J. Pharm.* **1994**, *103*, 37.

[2] X. Li, X. Deng, M. Yuan, C. Xiong, Z. Huang, Y. Zhang, W. Jia, *J. Appl. Polym. Sci.* **2000**, *78*, 140.

[3] R. T. Liggins, H. M. Burt, *Int. J. Pharm.* **2001**, *222*, 19.

[4] D. Lemoine, C. Francois, F. Kedzierewicz, V. Preat, M. Hoffman, P. Maincent, *Biomaterials* **1996**, *17*, 2191.

[5] M. L. Hans, A. M. Lowman, *Curr. Opin. Solid State Mater. Sci.* **2002**, *6*, 319 .

[6] P. B. O'Donnell, J. W. McGinity, *Adv. Drug Deliv. Rev.* **1997**, *28*, 25.

[7] H. Sah, *J. Control. Rel.* **1999**, 58, 143.

[8] M. van de Weert, W. E. Hennink, W. Jiskoot, *Pharm. Res.* **2000**, *17*, 1159.

[9] T. G. Park, W. Lu, G. Crotts, *J. Control. Rel.* **1995**, *332*, 211.

[10] J. Panyam, M. M. Dali, S. K. Sahoo, W. Ma, S. S. Chakravarthi, G. L. Amidon, R. J. Levy, V. Labhasetwar, *J. Control. Rel.* **2003**, *92*, 173.

[11] K. Letchford, H. Burt, *Eur. J. Pharm. Biopharm.* **2007**, *65*, 259.

[12] C. Cai, J. Lin, T. Chen, X. Tian, *Langmuir* **2010**, *26*, 2791.

[13] S. J. Holder, N. A. J. M. Sommerdijk, *Polym. Chem.* **2011**, *2*, 1018.

[14] J. S. Lee, J. Feijen, *J. Controlled Release* **2012**,*161*, 473.

[15] J. Z. Du, L. Fan, Q. M. Liu, *Macromolecules* **2012**, *45*, 8275.

[6] J. Hu, G. Zhang, S. Liu, ***Chem. Soc. Rev.***, **2012**, ***41***, 5933.

[17] Z. Ge, S. Liu, ***Chem. Soc. Rev.***, **2013**, ***42***, 7289.

[18] S. Chen, S. Cheng, R. Zhuo, *Macromol. Biosci.* 2011, *5*, 576.

[19] G. Gaucher, M. H. Dufresne, V. P. Sant, N. Kang, D. Maysinger, J. C. Leroux, *J. Controlled Release* **2005**, *109*, 169.

[20] N. Nishiyama, K. Kataoka, *Adv. Polym. Sci.* **2006**, *193*, 67.

[21] Y. Ohya, A. Takahashi, K. Nagahama, *Adv. Polym. Sci.* **2012**, *247*, 65.

[22] S. H. Kim, J. P. K. Tan, F. Nederberg, K. Fukushima, Y. Y. Yang, R. M. Waymouth, J. L. Hedrick, *Macromolecules* **2009**, *42*, 25.

[23] R. J. Pounder, H. Willcock, N. S. Ieong, R. K. O'Reilly, A. P. Dove, *Soft Matter* **2011**, *7*, 10987.

[24] Y. Ikada, K. Jamshidi, H. Tsuji, S. H. Hyon, *Macromolecules* 1987, *20*, 904.

[25] *H. Tsuji, Macromol Biosci*. **2005**, *5*, *569*.

[26] N. Kang, M. E. Perron, R. E. Prud'homme, Y. Zhang, G. Gaucher, J. C. Leroux, *Nano Lett.* **2005**, *2*, 315.

[27] K. Nagahama, Y. Mori, Y. Ohya, T. Ouchi, *Biomacrolecules* **2007**, *8*, 2135.

[28] Y. Zhu, T. Akagi, M. Akashi, ***Polym. J.* 2013, *45*, 560.**

[29] G. L. Peterson, *Anal. Biochem.* **1977**, *83*, 346.

[30] K. P. Ananthapadmanabhan, E. D. Goddard, N. J. Turro, P. L. Kuo, *Langmuir* **1985**, *1*, 352.

[31] T. Noda, Y. Morishima, *Macromolecules* **1999**, *32*, 4631.

[32] F. Wang, T. K. Bronich, A. V. Kabanov, R. D. Rauh, J. Roovers, *Bioconjugate Chem.* **2005**, *16*, 397.

[33] D. Brizzolara, H. J. Cantow, K. Diederichs, E. Keller, A. J. Domb, *Macromolecules* **1996**, *29*, 191.

[34] J. Kobayashi, T. Asahi, M. Ichiki, A. Oikawa, H. Suzuki, T. Watanabe, E. Fukada, Y. Shikinami, *J. Appl. Phys.* **1995**, *77*, 2957.

[35] H. Teuji, S. H. Hyon, Y. Ikada, *Macromolecules* **1992**, *25*, 2940.

[36] T. Okihara, M. Tsuji, A. Kawaguchi, K. Katayama, H. Tsuji, S. H. Hyon, Y. Ikada, *J. Macromol. Sci. Part B* **1991**, *30*, 119.

Chapter 3

Biodegradable NPs Composed of Enantiomeric γ-PGA-*g*-PLA Copolymers as Vaccine Carriers

3.1 Summary

The design of particulate materials with controlled degradation at desired sites is important in applications for drug/vaccine/gene delivery systems. Amphiphilic biodegradable polymeric NPs are promising vaccine delivery carriers due to their ability to stably maintain antigens, provide tailored release kinetics, effectively target, and function as adjuvants. In chapter 2, the ability of stereocomplex NPs composed of enantiomeric γ-PGA-*g*-PLA copolymers as protein delivery carriers were studied. In this chapter, the antigen-loaded stereocomplex NPs were successfully used for vaccines that can deliver antigenic proteins to dendritic cells (DCs) and elicit potent immune responses. The ovalbumin (OVA)-encapsulated isomeric and stereocomplex NPs were prepared for the study. These NPs were efficiently taken up by DCs, and also affected the intracellular degradation of the encapsulated OVA. The degradation of OVA encapsulated into the stereocomplex NPs was attenuated as compared to free OVA and the corresponding isomer NPs. Interestingly, immunization with OVA-stereocomplex NPs predominantly induced antigen-specific cellular

immunity. The crystalline structure of inner NPs consisting of PLA had significant impact on the degradation profiles of NPs and release/degradation behavior of encapsulated antigens, and thus the efficiency of immune induction. Our findings suggest that the γ-PGA-PLA stereocomplex NPs are suitable for protein-based vaccines that are used to induce of cellular immunity, such as for infectious diseases, cancer, allergies and autoimmune diseases.

3.2 Introduction

Vaccine adjuvants and delivery systems are used to improve the potency of the immune response to co-administered antigens.[1] Aluminum compounds (Alum) are the most widely used vaccine adjuvants and are employed in diphtheria, tetanus, pertussis, hepatitis B and pneumococcus vaccines. It has been proposed that Alum acts through the formation of a depot that induces the sustained release of the adsorbed antigen at the injection site.[2] Alum adjuvanticity is associated with enhanced antibody responses (humoral immunity). However, aluminum-based adjuvants can induce local reactions and fail to generate strong cell-mediated immunity. As a consequence, there is a great need to develop novel adjuvants and delivery systems for the next generation of vaccines.

Recently attention has been directed toward the utility of biodegradable NPs as delivery carriers for vaccines.[3],[4] A vaccine antigen is either encapsulated

within or immobilized onto the surface of the NPs. By encapsulating the antigenic component, NPs provide a method for delivering antigens which may otherwise degrade and diffuse rapidly upon injection. A key challenge in NP-based vaccine development is the efficient targeting of antigen-presenting cells (APCs), such as dendritic cells (DCs) and macrophages.[5] Exogenous particulate antigens are normally internalized by APCs, degraded and processed in the endosome/lysosomes, and presented on the MHC class II pathway, which is involved in T helper cell activation. In contrast, endogenous antigens are generally processed and presented via the MHC class I pathway, which is involved in cytotoxic T lymphocyte (CTL) activation (cellular immunity).[6] DCs have the unique capability to present exogenous antigens on MHC class I molecules. MHC class I-restricted antigen presentation by exogenous antigens is possible if the antigens escape from the lysosomes into the cytoplasm rather than being degraded in the lysosomes.[7] Therefore, it is suggested that not only the cell uptake process of the particulate antigens, but also the intracellular distribution and degradation of encapsulated antigens are important for the induction and regulation of antigen-specific immune responses. Moreover, it is expected that the desired immune response can be manipulated by controlling the process of antigen degradation in APCs.

Recently, the self-assembly of amphiphilic block copolymers or hydrophobically-modified polymers has been extensively studied in the field of drug delivery systems.[8],[9] In general, amphiphilic block/graft copolymers can self-assemble to form nano-sized micelles consisting of a hydrophilic outer shell and a hydrophobic inner core in aqueous solution. Amphiphilic block copolymers, such as PEG-*b*-PLA are very attractive for drug delivery applications.[10] These systems can be used to provide targeted cellular delivery of drugs, to avoid any toxic effects, and to protect therapeutic agents against enzymatic degradation (nucleases and proteases), especially in case of protein, peptide and nucleic acid drugs. Moreover, PLLA/PDLA-containing copolymers of various architectures were synthesized to form stereocomplex composites.[8] It has been reported that PLLA/PDLA mixtures in solution form stereocomplexs with distinctive physical and chemical stability due to their van der Waals interactions.[11],[12] It is well known that the physical and mechanical properties of a stereocomplex are largely dependent on its level of crystallinity. Application of this interaction for NP formation was first employed in micelle stabilization by Kang *et al.* with block copolymer micelles obtained through the self-assembly of equimolar mixtures of PEG-*b*-PLLA and PEG-*b*-PDLA in water.[13] These stereocomplex micelles possessed partially crystallized cores and exhibited kinetic stability superior to micelles prepared with isotactic or racemic polymers alone. Other groups have

used stereocomplex formation between enantiomeric PLA to fabricate or stabilize polymeric micelles or NPs with hydrophilic segments including PEG, PNIPAM, poly(L-histidine) or dextran.[14]-[17] The hydrolytic degradation of PLA is affected by different factors such as the chemical configuration, molecular weight, crystallinity and environmental conditions.[18] This suggests the possibility of tuning the degradation rate over a wide range of homopolymer PLLA, PDLA and stereocomplexed PLA composites.

In chapter 1 and chapter 2, biodegradable NPs composed of γ-PGA as a hydrophilic backbone and enantiomeric PLA as hydrophobic side chain were prepared. These γ-PGA-*g*-PLA copolymers can form NPs, and stereocomplex crystallites were formed in the case of the mixture of γ-PGA-*g*-PLLA and γ-PGA-*g*-PDLA copolymers.[19] Moreover, the stereocomplex NPs exhibit a lower CAC as well as stronger kinetic stability compared with the corresponding isomer NPs. We hypothesize that the crystalline structure of NPs would have significant impact on the degradation profiles of NPs and release/degradation behavior of encapsulated antigens, and thus the efficiency of immune induction. In this study, we investigated the efficacy of γ-PGA-*g*-PLA stereocomplex NPs on cellular uptake, intracellular degradation of protein encapsulated into the NPs *in vitro* and immune induction of protein-encapsulated stereocomplex NPs *in vivo*.

3.3 Experimental Section

Materials and reagents

L-lactide and D-lactide were purchased from Purac Biochem BV (Gorinchem, the Netherlands) and were re-crystallized twice from ethyl acetate prior to use. Poly(γ-glutamic acid) (γ-PGA, number average molecular weight: M_n = 75 kDa; molecular weight distribution: M_w/M_n = 2.0), stannous octanoate [$Sn(Oct)_2$], ovalbumin (OVA) and other chemicals were purchased from Wako Pure Chemical Industries and were used as received.

Synthesis and preparation of γ-PGA-PLA NPs

PLAs (M_n = 2.5 kDa) and γ-PGA-*g*-PLA copolymers (M_n of γ-PGA = 10 kDa) were synthesized as previously described.[19] The amphiphilic graft copolymers γ-PGA-*g*-PLLA and γ-PGA-*g*-PDLA were synthesized via a combination of ring opening polymerization and coupling reactions. The grafting degree of PLA, the number and hydrophobic content (%) of the PLAs in the copolymer were calculated from ^{1}H NMR (solvent DMSO-d_6). PLA content (wt. %) was calculated by following equation. PLA content (wt. %) = [(M_w of PLA × the number of grafted PLAs) / (M_w of γ-PGA-*g*-PLA)] × 100. In this study, γ-PGA-*g*-PLA copolymers with 5-6 PLA chains per γ-PGA (PLA content: 55-60 wt. %) were used. NPs composed of γ-PGA-PLLA (γ-PGA-*g*-PLLA NPs) and

γ-PGA-*g*-PLLA/γ-PGA-*g*-PDLA (γ-PGA-PLA stereocomplex NPs) were prepared by a precipitation and dialysis method. First, γ-PGA-*g*-PLLA, and an equal molar mixture of PLLA and PDLA copolymer was dissolved in DMSO, a solvent for both γ-PGA and PLA, to a concentration of 10 mg/ml. Then, phosphate buffer saline (PBS; 10 mM, pH 7.4) was added dropwise into the copolymer solution with vigorous stirring until the water content reached 50 vol. %. The solutions were transferred into a dialysis tube (MWCO: 1,000 Da) for dialysis against pure water. After dialysis, the particle size and distribution were measured by a dynamic light scattering (DLS) method using a Zetasizer Nano ZS (Malvern Instruments, UK).

X-ray diffraction (XRD) measurements

The XRD patterns of γ-PGA-*g*-PLA NPs were obtained from a RIGAKU RINT2000 apparatus. CuKα (λ=0.154 nm) was used as the X-ray source, and the patterns were measured at 40 kV and 200 mA with a Ni filter. The samples were examined at 2θ equal to 5-30°. The patterns were then curve-resolved into amorphous hollow and crystalline reflection peaks. After dividing the reflection peaks into homo-crystals (2θ = 17 and 19°) and stereocomplex crystals (2θ = 12, 21 and 24°), their crystallinities were estimated. In this study, γ-PGA-*g*-PLLA NPs (isomer) with homo-crystallinity of 40% and γ-PGA-*g*-PLA stereocomplex NPs with stereocomplex crystallinity of 58% were used.

Preparation of OVA-encapsulated γ-PGA-g-PLA NPs

To prepare the OVA-encapsulated γ-PGA-*g*-PLLA NPs (OVA-L NPs) and γ-PGA-*g*-PLA stereocomplex NPs (OVA-SC NPs), 2 mg of OVA was dissolved in 1 ml of PBS and slowly added into 1 ml of the DMSO solution of γ-PGA-*g*-PLLA isomers or mixture of γ-PGA-*g*-PLLA and γ-PGA-*g*-PDLA (10 mg/ml) with stirring. The resulting solution was centrifuged at 15,000 rpm for 10 min, rinsed with PBS twice, and re-suspended in PBS at a concentration of 10 mg/ml. OVA-encapsulated NPs (OVA-NPs) were added to DMSO to dissolve the NPs, and the OVA loading content was measured by the Lowry method. The morphology of the OVA-NPs was observed by scanning electron microscopy (SEM) (JEOL JSM-6701F) at 6 kV. A drop of the NP suspension was placed on a glass surface, which was fixed on metallic supports with carbon tape. After drying, the samples were coated with osmic acid.

In vitro release of OVA from γ-PGA-g-PLA NPs

The release experiment was carried out *in vitro* as follows: OVA-L NPs and OVA-SC NPs (1 mg/ml OVA, 10 mg/ml NPs) were suspended in 50 mM acetate (pH 5), phosphate (pH 7.4) and carbonate (pH 10) buffer, and were placed in a microtube at 37°C. At different time intervals, 100 μl samples were withdrawn and centrifuged at 15,000 rpm for 10 min. The amount of OVA released into the supernatant was then determined by the Lowry method.

Kinetics of the cellular uptake of OVA-NPs

Mouse bone marrow-derived dendritic cells (DCs) were generated, as previously reported.[20] FITC-labeled OVA (F-OVA) (Molecular Probes, Eugene, OR) was used to evaluate the uptake of F-OVA-NPs by DCs. To determine the kinetics of the F-OVA-NP uptake, the cells (1×10^5 cells/100 µ1) were incubated with a defined concentration of F-OVA alone, F-OVA-encapsulated γ-PGA-*g*-PLLA or γ-PGA-*g*-PLA stereocomplex NPs (F-OVA-L NPs or F-OVA-SC NPs) for 30 min at 37°C. F-OVA-NPs containing 100 µg of OVA per 1 mg of NPs were used. To quantify the amount of intracellular F-OVA-NPs, the cells incubated with F-OVA-NPs were washed thoroughly with PBS, and then dissolved with 0.5% Triton X-100 in 0.2 N NaOH solution for 1 h at room temperature, and then the fluorescence intensity of the lysates was measured by a fluorescence microplate reader (Fluoroskan Ascent FL, Thermo Fisher Scientific Inc., USA). The fluorescence incorporation was calculated as the amount of F-OVA uptake per cell.

Intracellular degradation of OVA encapsulated into the NPs

DQ OVA (Molecular Probes, Eugene, OR) was used to evaluate the intracellular degradation of the OVA-NPs. DQ OVA is a self-quenched OVA conjugate that exhibits fluorescence after degradation. DQ OVA-encapsulated NPs (DQ OVA-L NPs and DQ OVA-SC NPs) containing 100 µg of OVA per 1

mg of NPs were prepared by the same method as described above. DCs (5×10^5 cells/ml) were incubated with DQ OVA alone (100 μg/ml), DQ OVA-L NPs (3 μg/ml DQ OVA, 30 μg/ml NPs) or DQ OVA-SC NPs (1.5 μg/ml DQ OVA, 15 μg/ml NPs) for 30 min at 37°C. The amount of intracellular DQ OVA was regulated to be the same. After incubation, the cells were washed with PBS, and the NP phagocyted cells were incubated with PBS for up to 3 h at 37°C. After incubation for the prescribed time period, the cell-associated fluorescence (the fluorescence intensity of the degraded DQ OVA) was measured by flow cytometry (FCM) (Cytomics FC500, Beckman Coulter, US).

Immunization of mice with OVA-NPs

Female C57BL/6J (H-2K^b, 6 weeks old) mice were purchased from Charles River (Yokohama, Japan). All experiments were approved by Osaka University, and were carried out in accordance with the institutional guidelines for animal experimentation. C57BL/6J mice (3 mice per group) were immunized subcutaneously once or twice with PBS, OVA (10 μg), OVA (10 μg) mixed with incomplete Freund's adjuvant (OVA + IFA), OVA (10 μg) mixed with Alum (100 μg) (OVA + Alum), OVA-L NPs or OVA-stereocomplex NPs (10 μg OVA and 100 μg NPs) on days 0 and 7. On day 7 after the last immunization, spleen cells and blood were collected.

ELISPOT assay and ELISA

Interferon (IFN)-γ-producing cells were determined using an enzyme-linked immunospot (ELISPOT) kit for mouse IFN-γ (BD Biosciences). The spleen cells (4×10^5 cells/200 µl/well) isolated by density gradient centrifugation were either stimulated in vitro with 1 µg/ml of $OVA_{257-264}$ peptide (SIINFEKL) or unstimulated (negative control) in a 96-well ELISPOT plate. The plate was incubated for 24 h at 37°C. The IFN-γ-producing cells in the splenocyte populations were measured by a commercially available kit according to the manufacturer's instructions. The data were expressed as the mean spot forming units (SFU) per 4×10^5 cells ± standard deviation (SD). OVA specific IgG antibody levels in immunized mouse serum were measured by an enzyme-linked immnosorbent assay (ELISA) as previously described.[21]

3.4 Results and Discussion

Preparation of OVA-encapsulated γ-PGA-g-PLA NPs

In order to study the release behavior, cellular uptake, intracellular degradation and the induction of immune response by γ-PGA-*g*-PLA NPs, OVA-, F-OVA- or DQ OVA-encapsulated NPs were prepared. OVA dissolved in PBS were added to a γ-PGA-*g*-PLLA or γ-PGA-*g*-PLLA/PDLA mixture in DMSO solution. The obtained NPs were investigated for their protein loading capability. OVA,

F-OVA and DQ OVA were successfully encapsulated into the γ-PGA-*g*-PLLA and γ-PGA-PLA stereocomplex NPs. The encapsulation efficiency was found to be in the range of 50–60%, and the amount of encapsulated OVA per NP weight was almost the same, despite the differences in homopolymer and stereocomplex. In this chapter, OVA-NPs with an OVA loading of 100 μg per mg NPs were used for these experiments. The size of the OVA-encapsulated γ-PGA-*g*-PLLA (isomer) NPs (OVA-L NPs) and γ-PGA-*g*-PLA stereocomplex NPs (OVA-SC NPs) re-dispersed in PBS was measured by DLS. The OVA-SC NPs showed a monodispersed size distribution with a mean diameter of 440 nm (polydispersity index: PDI = 0.30) (Figure 3-1a). In contrast, the size distribution of OVA-L NPs exhibited two peaks (65 and 330 nm, PDI = 0.24). The formation of these NPs was accomplished due to the amphiphilic characteristic of γ-PGA-PLA. In the case of stereocomplex NPs, when the equimolar mixture of enantiomeric copolymers came into contact with the non-solvent PBS containing OVA under stirring, the association of the enantiomeric PLA chains took place very quickly before the solution goes into microscopic phase separation, and finally formed the stereocomplex cores of the NPs. It was considered that the stereocomplex formation plays an important role in controlling the size distribution of the NPs. The particle size was increased when OVA were encapsulated, and the size of the

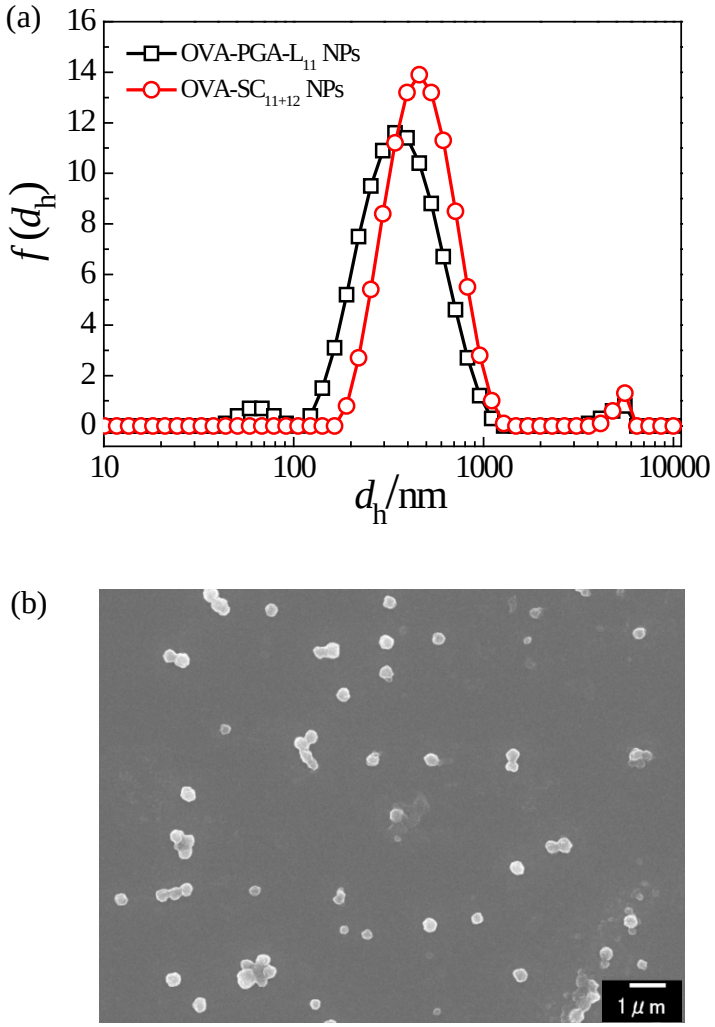

Figure 3-1. Size distribution of OVA-L NPs and OVA-SC NPs (a) and SEM images of OVA-SC NPs (b). OVA (2 mg/ml) dissolved in PBS was added to γ-PGA-*g*-PLLA or γ-PGA-*g*-PLLA/PDLA mixture (10 mg/ml) in DMSO solution at the same volume. After purification, the size of the NPs was measured in PBS by DLS.

OVA-NPs increased with increasing OVA content, likely due to an increase in swelling capacity due to the hydrophilic properties of OVA. Furthermore, it could be observed from the SEM observation that the OVA-SC NPs were spherical in shape (Figure 3-1b). The OVA-NPs had a strongly negative zeta potential (-25 mV) in PBS. The negative zeta potential was due to the ionization of the carboxyl groups of γ-PGA located near the surfaces.

Release behavior of OVA encapsulated into the γ-PGA-g-PLA NPs

To study the stability and protein release behavior, OVA-L NPs and OVA-SC NPs were simply suspended in buffers of pH 5, 7.4 and 10, and then the OVA release *in vitro* was determined. As shown in Figure 3-2, the OVA encapsulated into the both NPs were not released (less than 10%) at pH 5 and 7.4, even after 6 days. The OVA encapsulated into the γ-PGA-PLA NPs was stable under acidic and neutral conditions. In the case of NPs prepared from amphiphilic PLA-PEG block copolymers, hydrophobic interactions between the hydrophobic regions of protein and the hydrophobic PLA blocks were observed.[22] Therefore, it is suggested that hydrophobic interactions between the hydrophobic regions of OVA and the hydrophobic PLA part in the γ-PGA-PLA NPs is attributed to the stability of OVA-NPs. However, as the OVA-NPs are formed by amphiphilic γ-PGA-PLA graft copolymers, it is hypothesized that the core of the NPs is formed by not only the PLA, but also by the γ-PGA of the main chain. Thus,

γ-PGA may also be related to the interaction between the protein and the NPs. On the other hand, a significant amount of OVA was released in pH 10. The behavior of polyester degradation is controlled by a number of factors, such as pH, crystallinity, stereochemical structure, molecular weight, and presence of low molecular weight compounds.[23]-[25] The OVA was gradually released from the OVA-L NPs and OVA-stereocomplex NPs at pH 10, and the release percentage was about 20 and 50 % in the initial period within 8 h, respectively. A significant difference in the release profile between OVA-L NPs and OVA-stereocomplex NPs was observed during an early period (from 8 to 48 h) of incubation. The OVA release rate of OVA-L NPs was higher than that of OVA-stereocomplex NPs. It has been reported that no significant hydrolysis occurred when γ-PGA was incubated at pH 7 or pH 10 at 37°C. Even after 60 days of incubation at pH 7 or pH 10, only approximately 10% of the γ-PGA had been hydrolyzed.[26] These results suggest that OVA releasing from the NPs at pH 10 can be attributed to the degradation of PLA. The reason for the increased stability of OVA-stereocomplex NPs is suggested to be intermolecular crystallization of PLLA/PDLA, which results in larger number of tie chains between the crystallites and a more dense packing of the chains also in the amorphous phase.[27] Furthermore, the solubility of γ-PGA is increased upon increasing the pH, due to ionization of carboxyl groups containing γ-PGA. Thus,

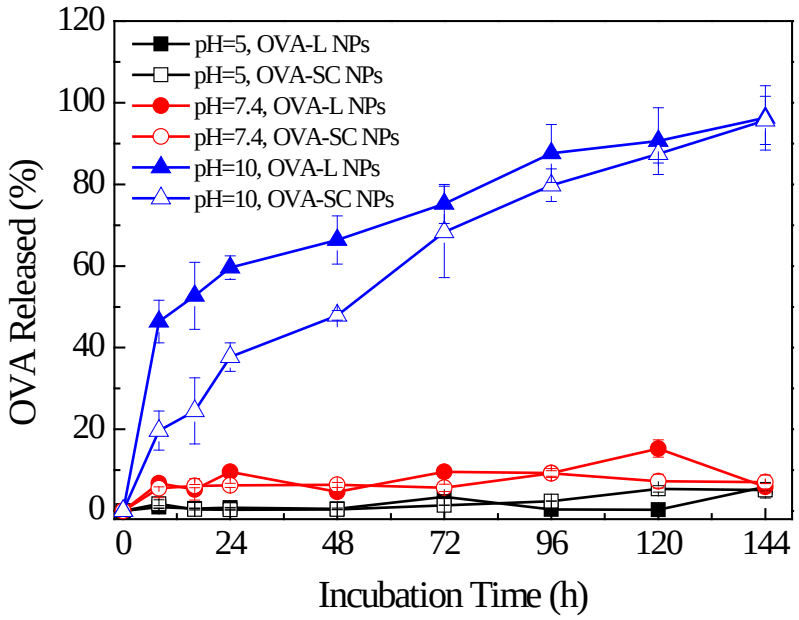

Figure 3-2. OVA release profiles of OVA-L NPs and OVA-SC NPs. The release of OVA from the NPs with an OVA content of 100 μg/mg NP was carried out at 37°C in pH 5 (square), pH 7.4 (circle) or pH 10 (triangle). The results are presented as means ± SD (n = 3).

OVA releasing from the NPs at pH 10 may be related to the solubility of γ-PGA backbone.

Uptake of F-OVA-NPs by DCs

To evaluate the uptake behavior of OVA-NPs by DCs, the cells were incubated with F-OVA NPs for the defined OVA and NP concentrations. To quantify the amount of F-OVA NPs taken up by DCs, the cells incubated with each concentration of F-OVA alone, F-OVA-L NPs or F-OVA-SC NPs were dissolved with a surfactant. The fluorescence intensity of the lysates was then measured. Figure 3-3 shows the cellular uptake kinetics of F-OVA NPs as a function of the concentration of F-OVA NPs or F-OVA alone. The uptake of F-OVA-L NPs and F-OVA-SC NPs increased with increasing concentration of the NPs, indicating that the uptake was dose dependent. F-OVA-stereocomplex NPs were more efficiently taken up than the F-OVA-L NPs. When 15 μg/ml (carrying 1.5 μg/ml F-OVA) of F-OVA-SC NPs, 30 μg/ml (carrying 3 μg/ml F-OVA) of F-OVA-L NPs or 100 μg/ml of F-OVA alone were pulsed, the same amount of OVA was taken up by the cells. In the case of F-OVA alone, an approximately 60-fold higher concentration was required to elicit a similar amount of intracellular OVA as compared to the F-OVA-SC NPs. These results showed that the γ-PGA-*g*-PLA NPs efficiently delivered the encapsulated protein into the cells. The reason why the uptake of F-OVA-SC NPs was higher than that

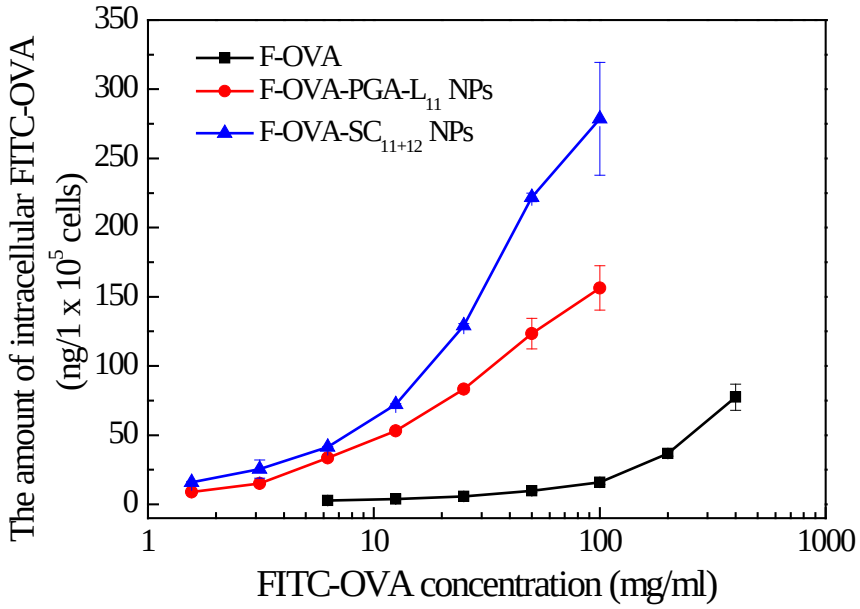

Figure 3-3. The dose dependency on the uptake of F-OVA-NPs by DCs. The cells were cultured with the indicated concentrations of F-OVA alone, F-OVA-L NPs or F-OVA-SC NPs for 30 min at 37°C. To quantify the amount of intracellular F-OVA, the cells were dissolved, and then the fluorescence intensity of the lysates was measured. The fluorescence incorporation was calculated as the uptake amount of F-OVA per cell (n=3).

of F-OVA-L NPs is not clear. The difference may be attributed to the size difference between these NPs.

In general, virus-sized particles (20-200 nm) are usually taken up by endocytosis via clathrin-coated vesicles, caveolae or their independent receptors. Larger-sized particles (0.5-5 μm) are taken up by macropinocytosis, and particles greater than 0.5 μm are predominantly taken up by phagocytosis.[28] It has been reported that DCs and macrophages are capable of ingesting polystyrene or PLA particles ranging from 50 nm to 5 μm in diameter, and that particles with a diameter of 500 nm or less are optimal for uptake by DCs.[29] In this study, 400 nm-sized F-OVA-NPs were taken up more efficiently than F-OVA alone by the DCs, and the uptake of F-OVA-NPs was inhibited at 4^{o}C, which suggests that F-OVA-NPs were phagocytosed mainly via the endocytosis pathway. In addition, the cytotoxicity of the OVA-L NPs and OVA-SC NPs was evaluated *in vitro* by a cytotoxicity test using DCs. The surviving cells after 24 h incubation were evaluated by the trypan blue exclusion assay. DC viability as a function of the concentration of NPs was investigated. The cellular viability was maintained at levels higher than 90% for both NPs, even at high concentrations (1 mg/ml). This implied that these γ-PGA-PLA NPs could be useful as protein carriers without any significant cytotoxic effects.

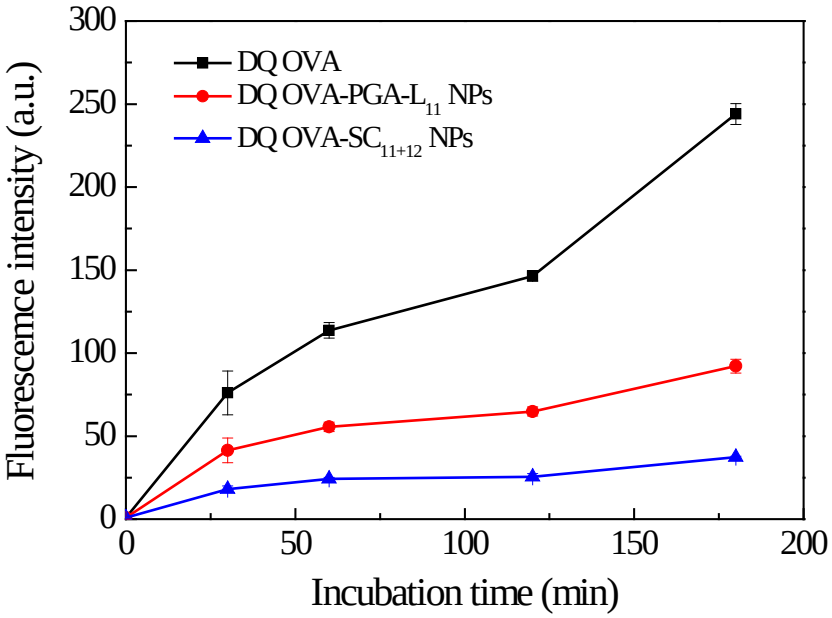

Figure 3-4. Intracellular degradation behavior of DQ OVA-NPs in DCs. The cells were incubated with DQ OVA alone (100 μg/ml) , F-OVA-L NPs (3 μg/ml DQ OVA, 30 μg/ml NPs) or F-OVA-SC NPs (1.5 μg/ml DQ OVA, 15 μg/ml NPs) for the indicated time periods at 37°C. The degraded DQ OVA (green) was observed using a FCM (n=3).

Intracellular degradation of OVA-NPs

The intracellular degradation of encapsulated OVA in the NPs was investigated using a pH-insensitive self-quenched OVA conjugate (DQ OVA) that exhibits bright-green fluorescence upon proteolytic degradation. DQ OVA-encapsulated γ-PGA-*g*-PLA NPs (DQ OVA-L NPs and DQ OVA-SC NPs) were prepared to study their degradation properties. DCs were incubated with DQ OVA alone, DQ OVA-L NPs or DQ OVA-SC NPs for up to 3 h at 37°C, and then observed using a FCM. Since the NPs influenced the amount of OVA uptake by DCs, DQ OVA alone and DQ OVA-NPs were pulsed into the cells under conditions where an equal amount of DQ OVA was taken up by the cells. Figure 3-4 shows intracellular degradation of DQ OVA in DCs as function of time. The uptake of DQ OVA alone (100 μg/ml pulsed) by the cells resulted in the early degradation of OVA. As the incubation time increased, the DQ OVA fluorescence became more intense inside the cells. As expected, the degradation of OVA encapsulated into the NPs was attenuated as compared to the free DQ OVA. Soluble DQ OVA was degraded much faster than the encapsulated DQ OVA. A difference in OVA degradation kinetics was observed between DQ OVA-L NPs and DQ OVA-SC NPs, the OVA degradation in the DQ OVA-SC NPs was less than in the DQ OVA-L NPs. These results indicated that the crystalline structure of stereocomplexed PLA in the NPs is an important factor for the degradation of

encapsulated protein. In this study, OVA-L NPs with homo-crystallinity of 40% and OVA-SC NPs with stereocomplex crystallinity of 58% were used. Therefore, the crystallinity itself may affect the degradation behavior of OVA.

Several studies have demonstrated that antigen-conjugated nano/microparticles affect the intracellular degradation of antigens. Cruz *et al.* reported that antigens encapsulated into poly(lactic-*co*-glycolic acid) (PLGA) particles were more slowly degraded within the lysosomal compartment of human DCs as compared to soluble antigen.[30] Tran *et al.* also reported that OVA-adsorbed polystyrene NPs (50 nm) showed the greatest degradation of OVA in DCs, and degradation was less evident for antigens adsorbed onto both 500 nm and 3 μm particles. The size of the polystyrene particles affected the phagosomal pH, and the different phagosomal pH profiles resulted in varying levels of OVA degradation.[31] We hypothesized that the differences in degradation due to stereocomplex crystallization of PLA could be attributed to differences in the intracellular degradation of OVA. In the case of γ-PGA-PLA NPs, the OVA degradation of DQ OVA-SC NPs was slower as compared to DQ OVA-L NPs. In general, PLA degradation has focused mainly on hydrolytic or enzymatic degradation. It has been reported that the biodegradation of PLA is strongly affected by its level of crystallinity and crystal forms.[18] Several reports showed that the crystalline part of the PLA was more resistant to degradation than the amorphous part, and that

the rate of degradation decreases with an increase in crystallinity.[32],[33] Only a few studies, however, deal with the degradation behavior of stereocomplexation crystallites. Tsuji *et al.* and Lee *et al.* reported that PLA stereocomplex has a higher hydrolysis-resistance compared with isomer PLLA or PDLA when it is hydrolyzed in PBS (pH 7.4) at 37°C or in enzyme.[34],[35] In Figure 3-2, the OVA encapsulated into the both NPs were not released at acidic pH (pH 5) in vitro, which is corresponding to pH of endosome. The result suggests that the encapsulated OVA are not released in the endosome by pH effect. It is thought that the retardation of the hydrolysis of PLA stereocomplex is mainly due to a strong interaction between L- and D-lactide unit sequences, which prevents the penetration of water or enzyme into the crystal structure. Based on these reports, the differences in the intracellular degradation of OVA might contribute to the high stereocomplex crystallization, the higher stability and hydrolysis-resistance of the OVA-stereocomplex NPs.

Induction of antigen-specific immune responses by OVA-NPs

The immune responses were investigated in mice after immunization with OVA-SC NPs. To evaluate the induction of cellular and humoral immunities, the mice were subcutaneously immunized 1 or 2 times at intervals of 7 days with OVA alone, OVA + IFA, OVA + Alum, OVA-L NPs or OVA-SC NPs. Splenocytes from the mice immunized with OVA-NPs were examined for their

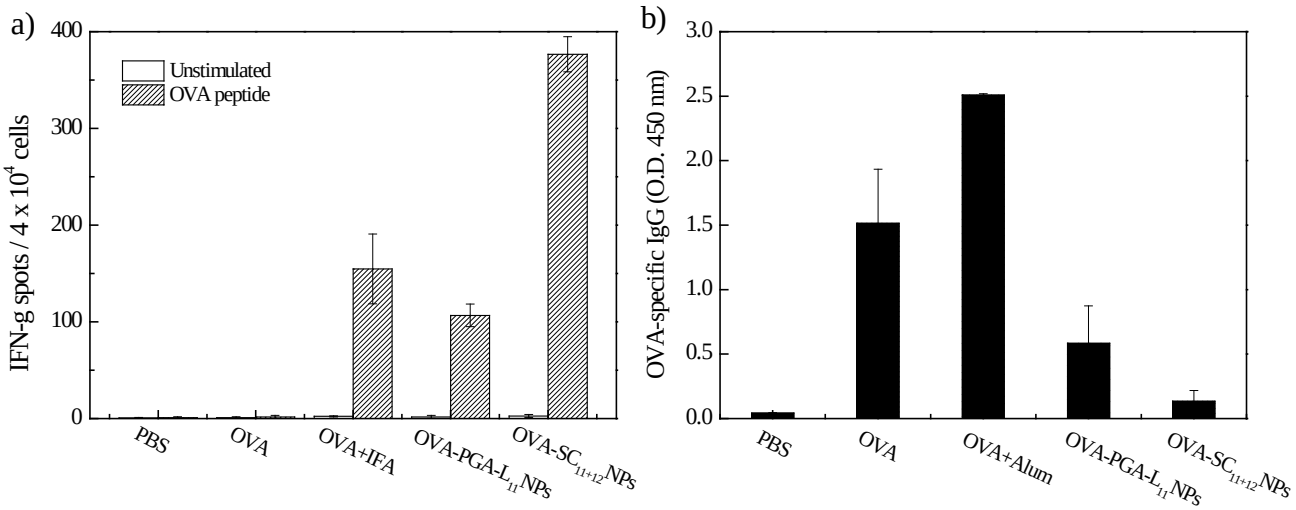

Figure 3-5. Induction of cellular and humoral immunities by immunization with OVA-NPs. (a) Mice were subcutaneously immunized one time with PBS, OVA (10 μg), OVA (10 μg) mixed with IFA (OVA + IFA), OVA-L NPs or OVA-SC NPs (10 μg OVA and 100 μg NPs). Splenocytes were obtained from the immunized mice on day 7 after the last immunization and stimulated with the $OVA_{257-264}$ peptide for 24 h. The number of IFN-γ-producing cells was measured by ELISPOT. The experiments were performed in triplicate. The results represent the means ± standard deviation (SD) from three mice per group. (b) OVA-specific IgG antibody responses in mice immunized two times with OVA, OVA mixed with Alum (OVA + Alum), OVA-L NPs or OVA-SC NPs. The levels of OVA-specific IgG antibody were measured by ELISA. Sera were diluted to 128 times. The absorbance was measured at 450 nm. Results are expressed as the mean ± SD in each group.

ability to induce IFN-γ-producing cells by ELISPOT assays. Figure 3-5a shows that the mice immunized with OVA-SC NPs demonstrated the efficient induction of IFN-γ-producing cells following in vitro stimulation with a CTL epitope peptide in the OVA. This activity was significantly higher than that observed for OVA + IFA. Interestingly, the induction level of antigen-specific cellular immunity by OVA-SC NPs was higher than that of OVA-L NPs. This result suggests that the induction level of antigen-specific cellular immunity could be enhanced by changing the crystalline structure of γ-PGA-PLA NPs. Next, OVA-specific antibody levels in serum were measured by ELISA. Mice immunized with OVA + Alum had high levels of anti-OVA IgG antibody in their sera (Figure 3-5b). On the other hand, the OVA-specific IgG antibody response by OVA-L NPs and OVA-SC NPs was lower than that of OVA alone, suggesting that OVA-NPs have a capacity to strongly induce cellular immunity rather than humoral immunity by subcutaneous immunization.

A major challenge in generating and manipulating immune responses is to create a vaccine system that can efficiently deliver antigens into the cytoplasm of APCs in order to induce antigen-specific cellular immunity. In this study, immunization of the mice with OVA-SC NPs predominantly induced OVA-specific cellular immune responses. It is assumed that the potent induction of the responses by OVA-SC NPs is attributed to antigen leakage from the

endosomes into the cytoplasm in the APCs, such as DCs and macrophages. In a previous study, we prepared biodegradable NPs composed of γ-PGA conjugated with L-phenylalanine (Phe) as the hydrophobic segment. Protein-encapsulated γ-PGA-*g*-Phe NPs efficiently delivered loaded proteins from the endosomes to the cytoplasm in DCs.[36],[37] The mechanism of endosome escape of the NPs is related their increased hydrophobicity when carboxylate ions of γ-PGA located near the surfaces become protonated at acidic pH values. The partial protonation of the γ-PGA carboxyl groups at endosomal pH were involved in pH-dependent membrane-disruptive activities.[38] In this study, OVA-SC NPs showed a strongly negative zeta potential in PBS. This negative charge of the NP surfaces is due to the carboxyl groups of γ-PGA. It is suggested the γ-PGA-*g*-PLA NPs have endosome-disruptive activity by the same mechanism as γ-PGA-*g*-Phe NPs. The NPs play a crucial role in the release of encapsulated OVA into the cytoplasm and subsequent antigen presentation via MHC class I. This behavior of the NPs might be related to their stability against hydrolytic and enzymatic degradation in the cells and at the injection site. Further studies are in progress to determine the cell trafficking behavior, antigen-presentation mechanisms and biodegradation in vivo of OVA-SC NPs.

3.5 Conclusions

In conclusion, polymeric NPs have attracted increasing interest as drug delivery carriers as well as for peptides, proteins, and DNA. Polymer complexes associated with two or more complementary polymers are widely used in potential applications in the form of particles. In general, electrostatic forces, hydrophobic interactions, hydrogen bonds, van der Waals forces, or combinations of these interactions are available as the driving forces for the formation of polymer complexes. In this study, the author focused on stereocomplexation of PLA to stabilize NPs consisting of enantiomeric γ-PGA-*g*-PLA graft copolymers for vaccine carriers. It is demonstrated that the crystalline structure of PLA in NPs is a key factor to control the release behavior and intracellular degradation of encapsulated protein. Importantly, the stereocomplexed NPs were able to deliver encapsulated antigen to DCs and regulate intracellular degradation of antigen and NPs, thereby modulating the immune response to the antigen. It is possible that γ-PGA-*g*-PLA stereocomplex NPs carrying vaccine antigens could provide a novel protein-based vaccine capable of inducing strong cellular immunity. These innovative vaccine delivery platforms could facilitate the development of effective vaccine therapy.

References

[1]. D. T. O'Hagan, N. M. Valiante, *Nat. Rev. Drug Discov.* **2003**, *2,* 727.

[2]. B. N. Lambrecht, M. Kool, M. A. Willart, H. Hammad, *Curr. Opin. Immunol.* **2009**, *21*, 23.

[3]. Y. Krishnamachari, S. M. Geary, C. D. Lemke, A. K. Salem, *Pharm. Res.* **2011**, *28*, 215.

[4]. A. E. Gregory, R. Titball, D. Williamson, *Front. Cell Infect. Microbiol.* **2013**, *3*, 1.

[5]. C. Foged, A. Sundblad, L. Hovgaard, *Pharm. Res.* **2002**, *19*, 229.

[6]. J. Banchereau, R. M. Steinman, *Nature* **1998**, *392*, 245.

[7]. A. Rodriguez, A. Regnault, M. Kleijmeer, P. Ricciardi-Castagnoli, S. Amigorena, *Nat. Cell Biol.* **1999**, *1*, 362.

[8]. S. Chen, S. X. Cheng, R. X. Zhuo, *Macromol. Biosci.* **2011**, *11*, 576.

[9]. A. Rösler, G. W. Vandermeulen, H. A. Klok, *Adv. Drug Deliv. Rev.* **2012**, *64*, 270.

[10]. G. Gaucher, M. H. Dufresne, V. P. Sant, N. Kang, D. Maysinger and J. C. Leroux, *J. Control. Releas* **2005**, *109*, 169.

[11]. Y. Ikada, K. Jamshidi, H. Tsuji, S. H. Hyon, *Macromolecules* **1987**, *20*, 904

[12]. D. Brizzolara, H. J. Cantow, K. Diederichs, E. Keller, A. J. Domb, *Macromolecules* **1996**, *29*, 191.

[13]. N. Kang, M. E. Perron, R. E. Prud'homme, Y. Zhang, G. Gaucher, J. C. Leroux, *Nano Lett.* **2005**, *5*, 315.

[14]. F. R. Kersey, G. Zhang, G. M. Palmer, M. W. Dewhirst, C. L. Fraser, *ACS Nano* **2010**, *4*, 4989.

[15]. S. H. Kim, J. P. K. Tan, F. Nederberg, K. Fukushima, Y. Y. Yang, R. M. Waymouth, J. L. Hedrick, *Macromolecules*, **2009**, *42*, 25.

[16]. R. Liu, B. He, D. Li, Y. Lai, J. Z. Tang, Z. Gu, *Macromol. Rapid Commun.* **2012**, *33*, 1061.

[17]. K. Nagahama, Y. Mori, Y. Ohya, T. Ouchi, *Biomacromolecules* **2007**, *8*, 2135.

[18]. H. Tsuji, *Macromol. Biosci.* **2005**, *5*, 569.

[19]. Y. Zhu, T. Akagi, M. Akashi, *Polymer J.* **2013**, *45*, 560.

[20]. X. Wang, T. Uto, K. Sato, K. Ide, T. Akagi, M. Okamoto, T. Kaneko, M. Akashi, M. Baba, *Immunol. Lett.* **2005**, *98*, 123.

[21]. T. Uto, X. Wang, K. Sato, M. Haraguchi, T. Akagi, M. Akashi, M. Baba, *J. Immunol.* **2007**, *178*, 2979.

[22]. P. Quellec, R. Gref, L. Perrin, E. Dellacherie, F. Sommer, J. M. Verbavatz, M. J. Alonso, *J. Biomed. Mater. Res.* **1998**, *42*, 45.

[23]. D. Cam, S.-h. Hyon, Y. Ikada, *Biomaterials* **1995**, *16*, 833.

[24]. I. Grizzi, H. Garreau, S. Li, M. Vert, *Biomaterials* **1995**, *16*, 305.

[25]. H. Tsuji, Y. Ikada, *J. Polym. Sci., Part A: Polym. Chem.* **1998**, *36*, 59.

[26]. F. Kesuo, G. Denis, S. Martin, *J. Environ. Polym. Degrad.* **1996**, *4*, 253.

[27]. H. Tsuji, Y. Ikada, *Polymer* **1999**, *40*, 6699.

[28]. S. D. Conner, S. L. Schmid, *Nature* **2003**, *422*, 37.

[29]. C. Foged, B. Brodin, S. Frokjaer, A. Sundblad, *Int. J. Pharm.* **2005**, *298*, 315.

[30]. L. J. Cruz, P. J. Tacken, R. Fokkink, B. Joosten, M. C. Stuart, F. Albericio, R. Torensma, C. D. Figdor, *J. Control. Release* **2010**, *144*, 118.

[31]. K. K. Tran, H. Shen, *Biomaterials* **2009**, *30*, 1356.

[32]. R. T. McDonald, S. McCarthy, R. A. Gross, *Macromolecules* **1996**, *29*, 7356.

[33]. H. Tsuji, S. Miyauchi, *Polym. Degrad. Stab.* **2001**, *71*, 415.

[34]. H. Tsuji, *Polymer 2000*, *41*, 3621.

[35]. W. K. Lee, T. Iwata, J. A. Gardella Jr, *Langmuir* **2005**, *21*, 11180.

[36]. T. Akagi, X. Wang, T. Uto, M. Baba, M. Akashi, *Biomaterials* **2007**, *28*, 3427.

[37]. T. Akagi, F. Shima, M. Akashi, *Biomaterials* **2011**, *32*, 4959.

[38]. T. Akagi, H. Kim, M. Akashi, *J. Biomater. Sci. Polym. Edn.* **2010**, *21*, 315.

Concluding Remarks

Preparation of stereocomplex NPs composed of enantiomeric γ-PGA-*g*-PLA copolymers as protein delivery carriers for vaccines that can deliver antigenic proteins and elicit potent immune responses is the research objective of this dissertation. The effects of the molecular weight of γ-PGA main chain, the grafting degree of the PLA side chain for the formation, stability and crystallinity of stereocomplex NPs were investigated in detail. The ability for antigen loading, delivery and the impact of crystalline structure of inner NPs on degradation profiles of NPs, release/degradation behavior of encapsulated antigens were evaluated. The results throughout this thesis are summarized as follows.

In chapter 1, the amphiphilic graft copolymers, γ-PGA-*g*-PLLA and γ-PGA-*g*-PDLA, consisting of a hydrophilic backbone of γ-PGA and hydrophobic side chains of enantiomeric PLLA or PDLA, were successfully synthesized. The number of enantiomeric PLA chains coupled onto γ-PGA can be controlled by changing the molar amount of PLA added into the reaction system. These γ-PGA-*g*-PLA copolymers could form NPs, and stereocomplex crystallites were formed in the case of the mixture of γ-PGA-*g*-PLLA and γ-PGA-*g*-PDLA copolymers having a relatively large number of PLA grafts.

In chapter 2, the effects of the molecular weight of the hydrophilic γ-PGA

main chain and the grafting degree of the hydrophobic PLA side chain for the formation, stability and crystallinity of NPs formed by isomers and the equal molar mixture of the isomers were investigated. The crystallinity of sterocomplex NPs can also be enhanced by using different preparation method. It is shown that stereocomplex NPs formed from acetonitrile have a higher crystallinity. Expected as a potential delivery system, the loading of model protein OVA into both the isomeric NPs and stereocomplex NPs were successfully achieved by both surface immobilization and physical encapsulation method.

In chapter 3, the efficacy of γ-PGA-*g*-PLA stereocomplex NPs on cellular uptake, intracellular degradation of protein encapsulated into the NPs *in vitro* and immune induction of protein-encapsulated stereocomplex NPs *in vivo* were investigated. The prepared OVA-encapsulated γ-PGA-*g*-PLA SC NPs can efficiently taken up by DCs, and also affected the intracellular degradation of the encapsulated OVA. The degradation of OVA encapsulated into the stereocomplex NPs was attenuated as compared to free OVA and the corresponding isomer NPs. Interestingly, immunization with OVA-SC NPs predominantly induced antigen-specific cellular immunity.

In this thesis, a kind of potential antigen delivery vehicle with higher thermodynamic and kinetic stability were successfully prepared from the

self-assembly of enantimeric γ-PGA-*g*-PLA graft copolymers. The author demonstrated that the crystalline structure of PLA in NPs is a key factor to control the intracellular degradation of encapsulated protein. Importantly, the stereocomplexed NPs were able to deliver encapsulated antigen to DCs and regulate intracellular degradation of antigen and NPs, thereby modulating the immune response to the antigen. It is possible that γ-PGA-*g*-PLA stereocomplex NPs carrying vaccine antigens could provide a novel protein-based vaccine capable of inducing strong cellular immunity. These innovative vaccine delivery platforms could facilitate the development of effective vaccine therapy.

List of Publications

Chapter 1

1. **Ye Zhu**, Takami Akagi, Mitsuru Akashi, "Preparation and characterization of nanoparticles formed through stereocomplexation between enantiomeric poly(γ-glutamic acid)-*graft*-poly(lactide) copolymers", *Polymer J.* **2013**, *45*, 560.

Chapter 2

2. **Ye Zhu**, Takami Akagi, Mitsuru Akashi, "Self-assembling stereocomplex nanoparticles by enantiomeric poly(γ-glutamic acid)-poly(lactide) graft copolymers as a protein delivery carrier", *Macromol. Biosci.* published online.

3. **Ye Zhu**, Takami Akagi, Mitsuru Akashi, "Peptide-conjugated biodegradable nanoparticles composed of stereoselctive complexes with poly(γ-glutamic acid)-poly(lactide) copolymers", in preparation.

Chapter 3

4. Takami Akagi, **Ye Zhu**, Fumiaki Shima, Mitsuru Akashi, "Biodegradable nanoparticles composed of poly(γ-glutamic acid)-poly(lactide) graft copolymers as vaccine carriers for induction of cellular immunity", *Biomater. Sci.* accepted.

Acknowledgements

I would like to express my sincere gratitude to Professor Mitsuru Akashi of Osaka University for his continuous guidance, helpful suggestions, and hearty encouragement through the course of this study.

In particular, I would like to express my gratefully appreciation to Associate Professor of Special Appointment (Takeda Pharmaceutical Company Limited Joint Research Chair) Takami Akagi in Osaka University for his continuous guidance, fruitful discussion and helpful suggestions to this work.

I would like to express my gratefully acknowledge to Associate Professor Toshiyuki Kida, Assistant Professor Michiya Matsusaki, Associate Professor of Special Appointment (Osaka University the Center for Advanced Medical Engineering and Informatics) Hiroharu Ajiro, and Invited Professor (University of Memphis Assistant Professor) Tomoko Fujiwara in Osaka University for their kind advice and helpful discussions.

I also express gratefully acknowledge to Professor Yoshihisa Inoue and Professor Nobuaki Kambe in Osaka University for their valuable comments and suggestions and Dr. Kyoko Inoue in of the analysis center in Osaka University for NMR measurement.

I also thank Dr. Koji Kadowaki, Miss Natsuko Hashimoto, Mr. Tomoaki

Hinoue, Mr. Masahiro Matsumoto, Miss Phassamon Piyapakorn, Mr. Fumiaki Shima, Mr. Akihiro Nishiguchi, Miss Paninee Chetprayoon, Mr. Chunyen Liu, Miss Yukie Takemoto, Miss Manami Shudo, Mr. Kazuya Takemura, Miss Mitsuyo Hamada, Mr. Takashi Yoshikai, Mr. Koki Azuma, Mr. Tatsuaki Ueyama, Mr. Shun Takahama, Mr. Daichi Hikimoto and Miss Chizuru Kogame as well as all members of Akashi laboratory for their support and kind assistance in these years.

Finally, I would like to express my heartfelt appreciation to my family and my friends for their thoughtful attention and continuous encouragements.

March 2014

Osaka University

Julia